Peak-to-Average Power Ratio (PAR) Reduction for Acoustic OFDM Systems

Guillem Rojo
Massachusetts Institute of Technology
Email: guillem@mit.edu

Advisor: Milica Stojanovic
Northeastern University
Email: millitsa@ece.neu.edu

September 10, 2009

ii

Contents

List of Figures

List of Tables

Acknowledgements

I would like to thank all the people that have helped me during these months in Boston. First of all, I want to thank Milica for giving me her best advices and for her patience reviewing all my documents, specially my writing ;). I want to thank Janice for her helpfulness with all the paper work, without her help I would have never been able to come to MIT. I would also like to thank everyone at the Sea Grant College for their support.

I would like to thank all the people who were working with us from Northeastern University. They have been giving my a lot of ideas for improving my work and my presentations! I have also learned a lot from them.

However, I would like to specially thank you the people who have been next to me during these months. First of all, my girlfriend who helped me a lot during the good and bad circumstances! I would like also to mention unforgettable friends (in order of appearance): Adri, Marina, Kathy, Jordi Martorell, Jordi Ribes, Guillem Palou and Héctor. But, I would specially like to thank my roommates: Josep Miquel, Guillem Crosas, Nik , Maria Andree (again ;)) and Marina. Without them, the experience at MIT would have been completely different.

Resumen

Las comunicaciones submarinas se remontan a la aparición de los primeros submarinos y la necesidad de comunicarse entre si. El "Gertrude" es conocido como el primer teléfono submarino, el cual consistía en un sistema de transmisión por voz a través de transductores. Sin embargo, era de corto alcance y poseía una escasa inteligibilidad.

Como en otros casos similares, el interés inicial por las comunicaciones subacuáticas fue por causas militares, pero poco a poco esta tecnología despertó interés en muchos otros campos. La investigación científica, el control sobre la polución en océanos o los sistemas de transmisión entre submarinistas son algunos ejemplos de las posibilidades que ofrecen las comunicaciones submarinas.

En general las ondas de radio convencionales no se propagan a través del agua. Esto es debido al aumento de la atenuación en el canal subacuático a altas frecuencias por este motivo las comunicaciones, en este medio, sólo se pueden establecer mediante ondas acústicas, cuya velocidad de propagación está limitada por la del sonido en el agua (1500 m/s), velocidad que es muy inferior a la de las ondas radioeléctricas. Por lo cual su tiempo de propagación es mayor y dificulta la transmisión de la información por el canal transmisor, y se produce una mayor sensibilidad del efecto Doppler.

Otro fenómeno importante en el canal subacuático es la propagación multi-camino que se produce por la refracción que se origina dentro del agua y por las múltiples reflexiones en el camino, tanto en el fondo del mar como en la superficie del océano. Tradicionalmente, se habían utilizado filtros ecualizadores en el dominio temporal para mitigar el efecto en la señal. Aunque con el paso del tiempo, la necesidad de aumentar la velocidad de transmisión y, por consiguiente, el ancho de banda hicieron insostenible la opción de ecualizar, porque para ecualizar se requerían filtros con un elevado número de coeficientes.

Con el objetivo de posibilitar el aumento de velocidad de transmisión, se introdujo la modulación OFDM (Orthogonal Frequency Division Multiplexing). Esta modulación, utilizada anteriormente en entornos de radio como redes inalámbricas WLAN o cuarta generación de telefonía móvil, consiste en dividir la banda de frecuencias en pequeñas subbandas, en las cuales la respuesta del canal puede modelarse como plana. El resultado es que la ecualización es mucho más sencilla debido a que OFDM combate la selectividad en frecuencia. La tecnología OFDM se consigue transmitiendo un símbolo en cada portadora las cuales están moduladas en frecuencias ortogonales.

La tecnología OFDM ofrece otras ventajas como son la fácil implementación a través de un módulo iFFT (inverse Fourier Fast Transform) y una gran eficiencia espectral debido a la ortogonalidad de las portadoras; por tanto, no se requieren bandas de guarda como en otras modulaciones. Pero también presenta grandes inconvenientes: la gran sensibilidad a los desplazamientos en frecuencia/fase y elevados picos en el dominio temporal que producen efectos adversos sobre los componentes no lineares de nuestro sistema. Por tanto, los elevados valores PAR ("Peak-to-Average") en el dominio temporal afectan a los amplificadores de potencia introduciendo distorsión.

El objetivo principal de este trabajo es la búsqueda, la implementación, la adaptación y la evaluación de técnicas de reducción de PAR para paliar la distorsión en los amplificadores no lineales. En la primera parte del trabajo se analizarán las diferentes técnicas existentes y su impacto sobre las comunicaciones subacuáticas.

A lo largo de la historia de las comunicaciones se han propuesto muchas técnicas prometedoras. Todas ellas proveen una reducción substancial en los picos de nuestra señal multiportadora, pero todas ellas presentan diferentes inconvenientes: algunas sacrifican velocidad de transmisión, otras incrementan la potencia final de nuestra señal, otras aumentan la probabilidad de error de bit (BER), otras acrecientan la complejidad computacional, etc.

Durante la primera parte de este proyecto final de carrera, se han estudiado y desarrollado las diferentes técnicas que han sido propuestas al largo del tiempo en la literatura sobre el tema. Los resultados demuestran que ninguna técnica específica es la perfecta solución para todos los sistemas multiportadores. De hecho, cada una de las técnicas debe ser cuidadosamente evaluada según los requerimientos del sistema. Además, en la práctica, deben ser considerados los efectos que producen los filtros transmisores, los convertidores D/A y el amplificador en transmisión para determinar qué técnica de reducción es la más adecuada.

El estudio de las diferentes técnicas existentes ha sido de vital importancia no sólo para saber los inconvenientes y ventajas de cada técnica, sino también para entender la metodología que se debe utilizar para resolver la problemática de PAR, y ha permitido desarrollar una técnica propia usando la metodología aprendida.

En la segunda parte del trabajo se plantea una técnica nueva para la reducción de los picos temporales de nuestra señal. La inexistencia de regulaciones legales para el espectro subacuático no pone impedimentos para transmitir fuera de nuestra banda de interés. Además, las bajas frecuencias de las ondas acústicas permiten que se pueda filtrar analógicamente. Basándose en los principios anteriores, este trabajo propone la reducción de PAR mediante la inserción de una señal fuera de banda que se encargará de cancelar los picos que presienta nuestra señal en tiempo.

En este trabajo se proponen dos implementaciones: una técnica que consiste un filtro LMS para calcular solución óptima de los coeficientes a insertar fuera de banda y una técnica subóptima que se basa en insertar tonos pseudo-aleatorios fuera de banda. Los resultados muestran que ambas técnicas nos ofrecen resultados significantes para la reducción de los indeseados picos.

La principal ventaja de esta técnica es que no consume ancho de banda, por consiguiente, no disminuye la velocidad de transmisión. Esto hace que sea una técnica muy atractiva para transmisiones en las cuales disponemos de un ancho de banda reducido, como es el caso de comunicaciones subacuáticas. Otra ventaja interesante es que no requiere distorsionar la señal para reducir el PAR, con lo cual se evitan problemas en la estimación y ecualización del canal.

Abstract

Orthogonal Frequency Division Multiplexing (OFDM) is an attractive modulation technique for underwater acoustic communications, where it has proven to be effective in combating the frequency-selective multipath distortion without the need for complex time-domain equalizers, thus offering simplicity of implementation. However, OFDM signals are characterized by large peak-to-average power ratios (PAR), which can reduce the system efficiency. To avoid the non-linear distortion in the transmit amplifier, the peak signal amplitude must be kept under a pre-specified limit, i.e. a back-off must be introduced, which reduces the average (useful) power.

PAR reduction techniques have been extensively studied for radio communication systems, and a number of solutions have been proposed (e.g., [8]- [9]). These techniques have varying PAR-reduction capabilities, power requirements, complexities, and bit rate losses. While they are applicable to acoustic systems, we take a different approach that aims to capitalize on the fundamental differences between the acoustic and radio systems.

Acoustic systems are confined to low frequencies due to the propagation losses, while further band-limiting occurs naturally in the transducer. The transducer thus acts as an analog filter in the final stage of transmission. While otherwise undesirable, this filtering effect can be exploited towards PAR reduction. Namely, our method consists of inserting out-of-band tones which are computed to minimize the peak amplitude of the OFDM signal. The resulting signal, consisting of the original signal plus the out-of-band tones, is amplified avoiding the non-linear range of the device, and fed to the transducer. The additional tones are rejected by transducer filtering, and the signal transmitted into the channel occupies only the bandwidth of the transducer. Since the tones are inserted out of the data bandwidth, this scheme does not reduce the total bit rate. The absence of frequency regulations in underwater communications also allows some spillage of the signal out of band. Note that if this is undesirable, additional filtering can be performed (digitally, before amplification).

System optimization involves selection of the out-of-band tones, which can be modulated using symbols from the same alphabet as the information-bearing symbols, or a different one. For a given number and location of the out-of-band tones, each selection of control symbols will result in a different PAR. Finding the optimal control sequence can fortunately be formulated as a convex problem and solved exactly [8]. The existence of the optimal solution is significant for assessing the performance bounds, but a practical solution must aim for lower computational complexity. Two approaches are proposed in this work. First, we propose an gradient algorithm which computes the optimal solution for the inserted tones. Then, we introduce a simple, albeit sub-optimal alternative for selecting the control sequence. It is based on generating a pre-determined number of random sequences, evaluating their PAR, and choosing the best candidate.

We study the impact of the number of candidate sequences, their constellation, as well as the location of the out-of-band tones. Numerical analysis shows that a relatively small number of candidate sequences suffice to bring the performance close to the optimal. Higher constellations offer better PAR reduction at the expense of a longer search. Finally, the best tone allocation appears to be at the high frequency end, close to the data bandwidth.

History

Undersea acoustic communications dates back to the development of the first submarines and the need to communicate them. The "Gertrude" was the first underwater telephone. It was an original system which simply transmitted voice directly with the aid of transducers and was notorious for short range and poor intelligibility. This system is still used on submarines around the world, both large military systems and small industrial or scientific submersibles.

The past three decades have seen a growing interest in underwater acoustic communications. The advent of digital communications makes possible develop further systems for complex channels such as the underwater acoustic channel. In particular, the available throughput in non-compensated delay-spread channel is limited to be less than $1/D_s$, where D_s is the length of the delay spread.

An early effort during the 1970s by Williams and Battestic was reported in [10]. Their paper explains a system to compensate the multipath propagation that would allow the bit rate to be faster than $1/D_s$. Williams and Battestic were researching propagation of low frequencies (around 300 Hz) in a medium range (270-450 km) in Atlantic Ocean. Their system provides a compensation that effectively reduces the effect of the multipath propagation.

In recent years, underwater communications have received more attention. Apart from military applications, underwater communications has been also used for coastline protection, monotirizing pollution in environmental systems, communication between divers, remote control in off-shore oil industry, among others. Because of that, underwater communications has been one of the main research lines of the Sea Grant College. Through their research, education and outreach activities, Sea Grant has helped position the United States as the world leader in marine research and sustainable development of coastal resources. Sea Grant activities exist at the nexus of local, state, national and sometimes international interests.

Finally, I recommend a series of review papers [11–13] which provide an extensive analysis about the developments in underwater acoustic communications during the last decade.

Chapter 1

Underwater communications systems

Acoustic communications are the most common physical layer in underwater communications. In an underwater environment, radio waves propagate only at low frequencies (50-300Hz), which require large antennas and high transmission power. Optical waves do not suffer from high attenuation in the blue range, but are affected by scattering. In addition, optical waves can only be transmitted in short distances due to losses caused by the precision in the laser beam.

1.1   Acoustic propagation

Underwater acoustic communications is one of the most challenging communication media. Underwater channels impose many constraints that affect the design of the wireless network. For instance, they are characterized by a path loss that depends on signal frequency and distance between the receiver and the transmitter. In addition, the parameters which characterize our channel are temporally varying due to the atmospheric changes and transmitter/receiver motion.

The main characteristics of the underwater acoustic channel are summarized in the chapter.

1.1.1   Attenuation

Attenuation is high both at very low frequencies and at high frequencies, which limits the available bandwidth. The path loss that occurs in an underwater channel over a distance l for a signal of frequency f is given by:

$$A(l, f) = (l/l_r)^k \cdot a(f)^{l-l_r} \tag{1.1}$$

where k denotes the spreading factor , l_r is the reference distance and $a(f)$ is the absorption coefficient, which is expressed empirically using the Thorp's formula as:

$$10 log a(f) = 0.11 \frac{f^2}{1 + f^2} + 44 \frac{f^2}{4100 + f^2} + 2.75 \cdot 10^{-4} f^2 + 0.003 \tag{1.2}$$

where f is in kHz. This formula is valid for frequencies above a few hundred Hz. The absorption coefficient increases rapidly with frequency (Fig. 1.1), thus imposing a cutoff on the available bandwidth for a given distance. Even though reduced bandwidths are commonly used, the system is inherently wideband due to low carrier frequencies which are employed in acoustic communications.

1.1.2   Noise

The ambient noise in acoustic channel can be modeled through four basic sources: turbulence, shipping, waves and thermal noise [14]. The following formulas give the power of spectral function density (p.s.d.) and

1
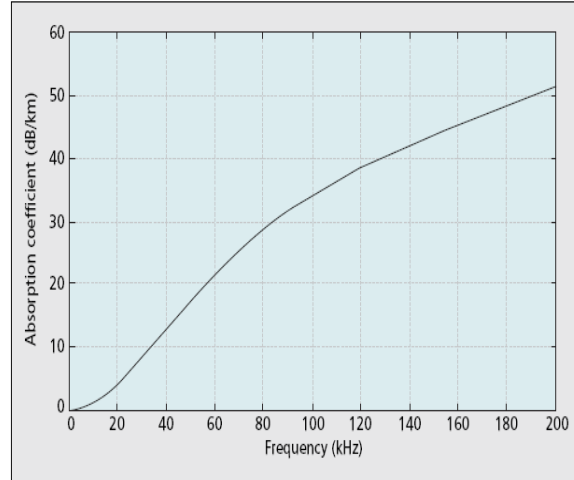
Figure 1.1: Absorption coefficient, $10 log a(f)$ in dB/Km.

they are expressed in dB re μPa per Hz as a function of frequency in kHz:

$$10logN_t(f) = 17 - 30logf$$
$$10logN_s(f) = 40 + 20(s - 0.5) + 25logf - 60log(f + 0.003) \tag{1.3}$$
$$10logN_w(f) = 50 + 7.5w^{\frac{1}{2}} + 20logf - 40log(f + 0.4)$$
$$10logN_{th}(f) = -15 + 20logf$$

where the shipping activity s ranges from 0 to 1, for low and high activity, respectively, and w is the wind speed measured in m/s. Turbulence noise influences only the very low frequencies , $f < 10Hz$. Noise caused by shipping is dominant in the frequency region 10-100 Hz. Surface motion caused by wind-driven waves is the major contributor to the noise in the frequency region 100 Hz-100 kHz which is our frequency of interest in acoustic communications. Finally, the thermal noise becomes dominant for f>100 kHz, out of our interest bandwidth. For more detailed information see [14].

Most of the sources may be described as having a continuous spectrum and Gaussian statistics and the p.s.d of the overall ambient noise can be approximated by a power spectral density that decays at approximately 18 dB/decade [14]. The approximation is shown in the Fig. 1.2.

1.1.3   Multipath propagation

A common phenomenon in underwater acoustic communications is the multipath spreading. A transmitted signal follows different paths to arrive to the receiver, thus causing the reception of different echoes of the same signal, but with different amplitude and phase. Multipath is due to sound reflection at the surface, bottom or objects and sound refraction in the water (See Fig. 1.3). The refraction is a result of sound speed variation with depth, is not common in shallow water communications. The channel impulse response can be written as

$$h(t) = \sum_{p=0}^{P} h_p \delta(t - \tau_p) \tag{1.4}$$

τ_p and h_p are the delay and attenuation of each path. Nonetheless, as stated before, the path gain has a frequency-distance dependency and can be modeled as a low pass filter.

Multipath dispersion implies frequency-selectivity which must be equalized at reception in order to de-modulate the signal. Orthogonal Frequency Division Multiplexing (OFDM) offers an effective way to avoid
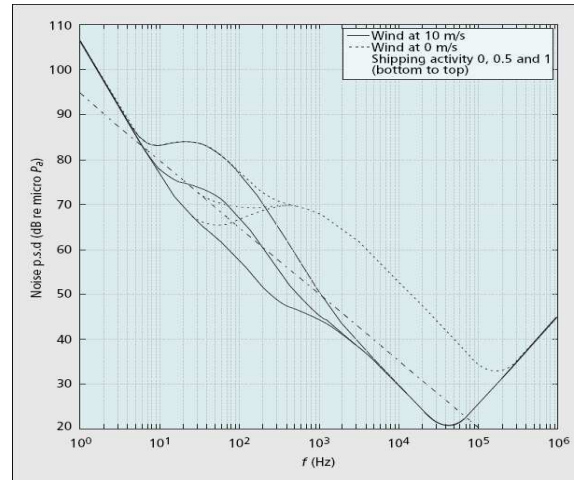
Figure 1.2: Power spectral density of the ambient noise.

inter-symbolic interference (ISI) caused by multipath spread [15].
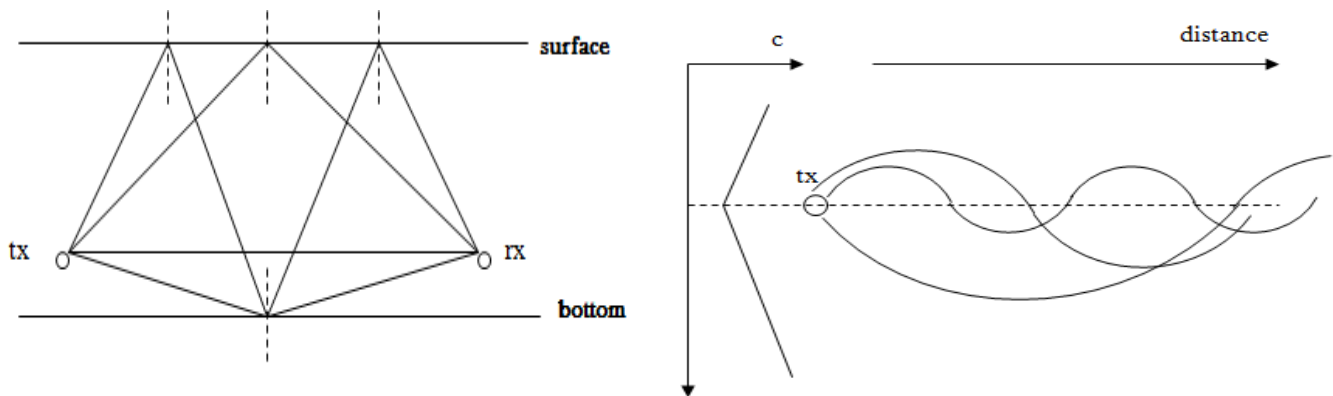
Figure 1.3: On the left, the different paths of the signal which arrive to the receiver. On the right, the effect of the sound refraction in the different paths.

1.1.4 Propagation delay

There is a long propagation delay in underwater acoustic communications due to the low speed of sound (1500 m/s). The high latency in the network makes difficult to use feedback information at the transmitter. Channel coherence time below 100 ms has been observed in underwater communications which is lower than our Round Trip Time (RTT). I.e, taking into account the speed of sound is 1500 m/s, that would imply an RTT of a half second in a communication of 750m.

1.1.5 Doppler Effect

Motion of the transmitter or receiver contributes additional changes in the channel response. The Doppler effect is observed in our received signal, which causes frequency shifting as well as frequency spreading.

It is well known that the Doppler effect is proportional to $a = v/c$ which is the ratio of relative transmitter-receiver motion to the speed of sound. In contrast with radio wireless communications, the speed of sound

is 1500 m/s. It does not neglect the Doppler effect. In addition, the autonomous unmanned vehicles are always subjected to drifting with waves, currents and tides. For example, a stationary system experience with an unintentional motion of 1,02 m/s (2 knot) results in a Doppler Effect of $a = 6.8 \cdot 10^{-4}$. This value cannot be neglected during the symbol synchronization in the transmission, in contrast with radio wireless communications which have values of a with an order of magnitude around 10^{-7}.

As a result, the delay suffered by the signal changes during the transmission, which might change the duration of the signal observed at the receiver. In fact, at the receiver, the duration of transmission is $T/(1+a)$ and the bandwidth $B(1+a)$, where T and B are the pulse duration and bandwidth of the transmitted signal, respectively. This effect is known as motion-induced Doppler spreading. Also a frequency offset $a \cdot f_k$ occurs for a signal of frequency f_k. This effect is known as the Doppler shifting. Non-negligible motion-induced Doppler shifting and spreading forces the need for delay synchronization and phase tracking. In the case of multicarrier systems, the Doppler Effects creates a nonuniform Doppler distortion across the signal bandwidth as it is shown in the Fig. 1.4.
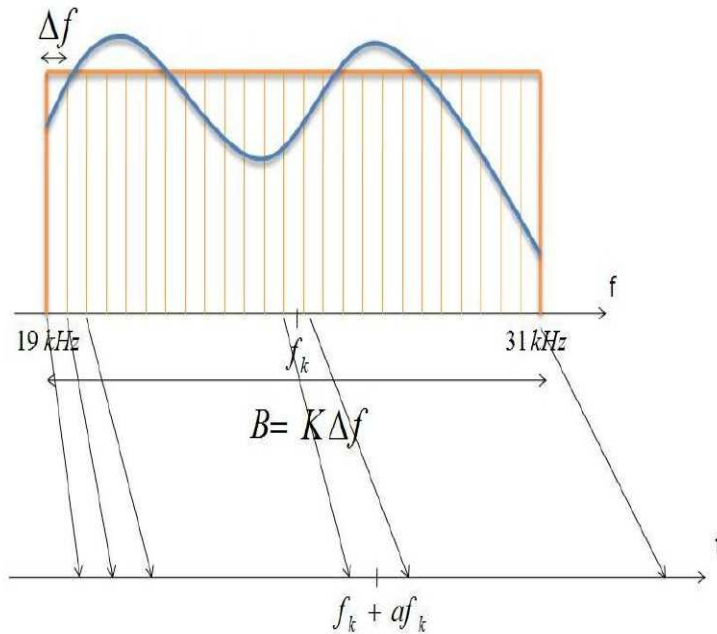
Figure 1.4: OFDM and non-uniform compensation produced by Doppler

1.2   Resource allocation

In contrast to radio spectrum frequency, the underwater channel is not regulated yet by Federal Commission of Communications (FCC). However, taking into account both acoustic path characterization and the ambient noise, the frequency allocation possibilities are reduced.

In this section, the frequency allocation methodology is introduced in order to decide the impact of changing the center frequency f_c and its corresponding bandwidth B.

1.2.1 Definition of optimal frequency

The narrow-band signal to noise ratio (SNR) is given by

$$SNR = \frac{S(f)\Delta f/A(l,f)}{N(f)\Delta f} = \frac{S(f)}{N(f) \cdot A(l,f)} \tag{1.5}$$

where $S(f)$ is the power spectral density of the transmitted signal and Δf is a narrow band around f. Taking into account the models, which described the noise and the absorption factor, $1/N(f) \cdot A(l,f)$ is plotted in the Fig. 1.5. It is observed from the figure that given a certain transmission distance l, it exists an optimal frequency $f_0(l)$ for which the maximal narrow-band SNR is achieved.
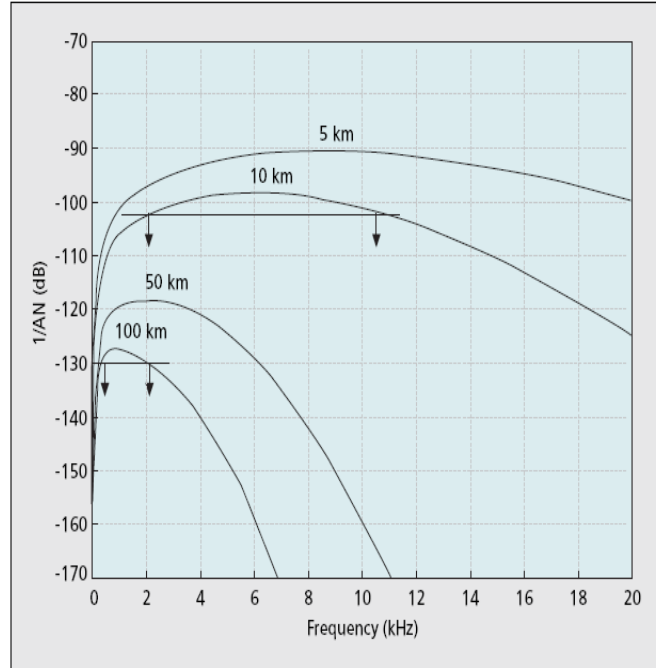
Figure 1.5: Frequency-domain part of the narrow-band SNR, $1/A(l,f)N(f)$, for different transmission distances (spreading factor $k = 1.5$)

1.2.2 Bandwidth definition

We define the 3 dB bandwidth $B_3(l)$ as the range of frequencies around $f_0(l)$ for which $A(l,f)N(f) < 2A(l,f_0)N(f_0)$. The achievable bandwidth is depending on the transmission distance l. Consequently, when a transmission distance is reduced, the bandwidth is higher. This dependance is not reported in radio communications. In Fig.1.6, the different available bandwidth as a function of the distance is plotted.

1.2.3 Transmission Power

Assuming that the transmitted signal p.s.d is flat across the 3 dB bandwidth, the transmission power necessary to provide a target SNR_0 at a distance l is given by the expression:

$$P(l) = SNR_0(l) \cdot B_3(l) \cdot \frac{\int_{B_3(l)} N(f)df}{\int_{B_3(l)} A^{-1}(l,f)df} \tag{1.6}$$
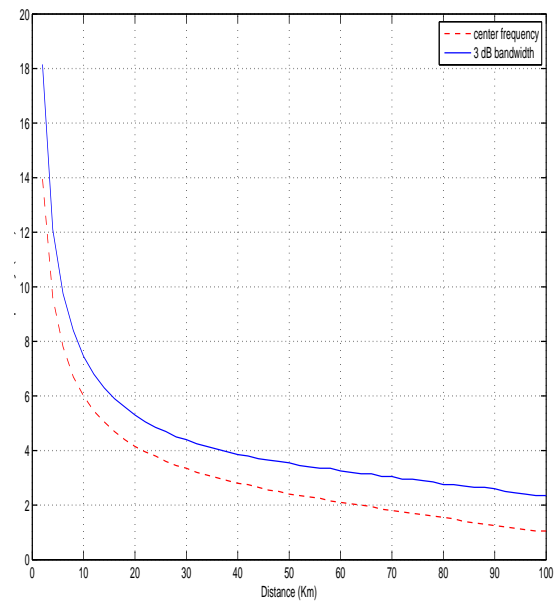
Figure 1.6: Optimal center frequency and the 3 dB acoustic bandwidth as functions of distance [1].

Chapter 2

Orthogonal Frequency Division Multiplexing

2.1   Introduction to OFDM

Achieving Data Rates that approach capacity over a noisy linear channel with memory, requires sophisti-cated transmission schemes that combine coding and shaping with modulation and equalization. While it is known that single-carrier system employing a minimal-mean-square error decision feedback equalizer can be, in some cases, theoretically optimum [16], the implementation of this structure in practice is difficult. In particular, the required lengths of the transmitted pulse shaping filters and the receiver equalizers can be long. An alternative to this scheme that is more suitable for a variety of high-speed applications on difficult channels is the use of multicarrier modulations, which is also optimal for the infinite-length case. The term of multicarrier modulations includes a number of schemes whose main characteristic is the decomposition of any wideband channel into a set of independent narrowband channels. Within this family, the most common used modulations are the Discrete MultiTone (DMT) and Orthogonal Frequency Division Multiplexing (OFDM) which are based on the Discrete Fourier Transform, resulting in an easy and implementable solution with a high performance.

OFDM is a multicarrier transmission in which the available bandwidth is divided among different orthog-onal subbands. The information of the user is transmitted parallel in these narrowband subbands. With this technique, a frequency selective channel is converted into several flat fading channels.

2.1.1   An OFDM system

The input signal is serial-to-parallel converted into K streams $d_k(n)$, $k = 0, ..., K-1$, among which the pilot tones are usually included to estimate the channel response at the receiver. These K symbols are transmitted in parallel onto K orthogonal subcarriers. The OFDM symbol is K times greater than a single-carrier system.

Afterwards, a guard band interval is added in order to mitigate the effect of ISI caused by the multipath effect which was explained in chapter 1. This guard band has to be longer than the delay spread of the underwater channel. Two types of guard band exist: Cyclic Prefix (CP) which consists in copying the last IFFT-precoded samples at the begin of the OFDM block and Zero Padding (ZP) which is based on appending zero samples after it.

The transmitted signal at the channel is

$$x_n(t) = \sum_{k=0}^{K-1} d_k(n) \exp^{j2\pi k \Delta f(t-nT')} g(t - NT') \tag{2.1}$$
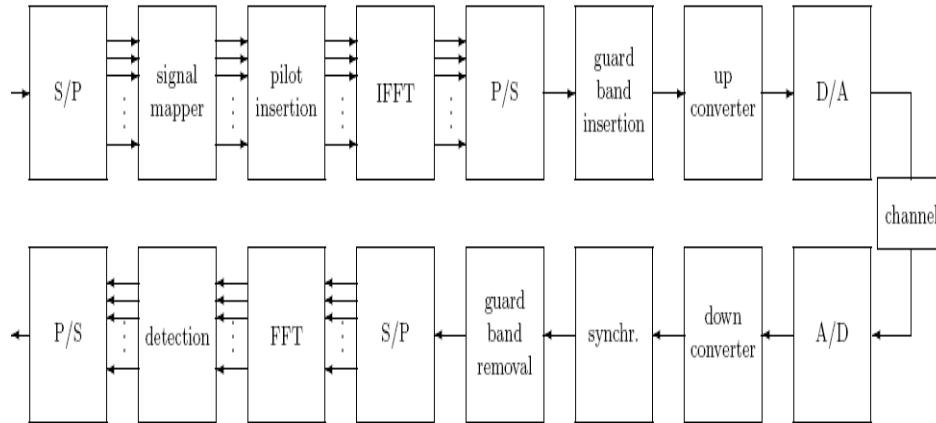
Figure 2.1: OFDM scheme: transmitter and receiver for CP-OFDM and ZP-OFDM.

where $g(t)$ is a rectangular pulse in time with unit amplitude and duration T'. In the case of ZP, $T' = T$ where T is the symbol period which has to be $T = 1/\Delta f$ in order to make the subcarriers orthogonal, as it is shown in the equation 2.2. In the case of CP, $T' = T + T_g$ where T_g is the guard band.

$$< \phi_k(t), \phi_l(t) > = \int_0^T e^{j2\pi(k-l)\Delta f t} dt = \frac{e^{j2\pi(k-l)} - 1}{2\pi\Delta f(k-l)} = \delta(k-l) \tag{2.2}$$

Subsequently, the entire signal is up-converted and it has the following expression

$$s(t) = \Re \left\{ \sum_n x_n(t) e^{j2\pi f_0 t} \right\} \tag{2.3}$$

In many papers the number of time samples of an OFDM block is $N_s = K$ and the number of frequency is K. Hence, if the sampling frequency $f_s = 1/T_s$ and $N_s = f_s T$, then the discrete signal produced at the transmitter is

$$s(mT_s) = \Re \left\{ \sum_n \sum_{k=0}^{K-1} d_k(n) e^{j2\pi km/N_s} \right\} \tag{2.4}$$

The symbol rate of the transmitted signal is $R/(T + T_g)$ symbols per second and total bandwidth is $B = K\Delta f$. As a result, the bandwidth efficiency is $R/B = T/(T + T_g)$ sps/Hz. Taking into account the total bandwidth to verify the Nyquist theorem, the sampling frequency has to be $f_s = N_s/T = N_s B/K \geq 2B$.

When it comes to choosing the number of subcarriers K, different parameters must be evaluated: T has to be larger than T_g, which must be greater than the delay spread to mitigate the ISI, to have spectral efficiency. Hence, it implies a large number of subcarriers K. On the other hand, the carrier spacing Δf must be greater than Doppler shifting f_d to avoid ICI. That implies a low number of subcarriers. Therefore, there is a tradeoff between spectral efficiency and inter-carrier interference sensitivity.

Finally, to recover the signal, the FFT is implemented at the receiver. Each symbol can be detected separately, errors caused by strong channel attenuation or noise in specific subbands can be prevented, thus making the system robust to narrowband interference and distortion. Different modulation can be applied depending on the frequency response of the channel. However, due to the high latency caused by the low speed of sound this inherent flexibility cannot be employed for underwater communications.

In summary we can say that the main advantages of OFDM are

- Robustness against multipath fading and inter-symbol interference and narrowband interference

- High spectral efficiency (no side bandwidth required for system operation).

- Low receiver complexity due to the simpler frequency domain equalization, as well as , simpler implementation using IFFT/FFT.

- Inherent flexibility in the system which allows:

  adaptive bit and power loading,

  adaptive modulation and coding,

  adaptive subcarrier allocation,

  space-time processing, MIMO.

and its main disadvantages are

- Sensitivity to frequency offset and phase noise, which are sources of inter-carrier interference. It may arise either from motion-induced Doppler or from the mismatch in the frequencies of the total oscillators do not occur in all-digital implementation, which is the one used for OFDM signals.

- High Peak-to-Average power Ratio (PAR) of the transmitted signal resulting in:

  nonlinear distortions of power amplifiers,

  BER performance degradation,

  energy spilling into adjacent channels.

Therefore, Orthogonal Frequency Division Multiplexing (OFDM) is an attractive modulation technique for underwater acoustic communications, where it has proven to be effective in combating the frequency-selective multipath distortion without the need for complex time-domain equalizers, thus offering simplicity of implementation. However, its disadvantages introduce problems when OFDM is implemented in a real system. This thesis aims to study the different possible solutions in order to mitigate the high Peak-to-Average power Ratio (PAR).

Chapter 3

Peak-to-average Ratio Power

3.1   Introduction to PAR

Orthogonal frequency division multiplexing (OFDM) has been considered for underwater communications as a low-complex alternative to single carrier broadband modulation [15, 16]. It has proved to be an effective technique to combat multipath dispersion without the need of complex time-domain equalizers.

One of the major drawbacks of OFDM modulation is its high peak-to-average power ratio (PAR). Large PARs occur when symbol phases line up so as to constructively form peaks in the time-domain signal. Since the peak transmission power is limited, either by regulatory or hardware constraints, the average power must be reduced, leading to a loss in performance relative to the constant amplitude modulation techniques.

Furthermore, an OFDM signal is very sensitive to non-linear distortion, which causes spectral growth of the multicarrier signal in the form of intermodulation products among subcarriers. Non-linearity is present in the power amplifier at transmitter, and to avoid it, the signal should be kept within the linear region. In addition, large PAR leads to more complex analog-to-digital and digital-to-analog converters because signals with constant envelope are desired for digitalizing.

When a signal is transmitted through a nonlinear device, such as a high-power amplifier (HPA) or a digital-to-analog converter (DAC), a high peak signal generates out-of-band energy (spectral growth) and in-band distortion (constellation tilting and scattering). An example of these consequences in the constellation is plotted in Fig. 3.3.

These degradations may affect the system performance severely. In order to understand the effects, the nonlinear behavior of an HPA must be characterized by amplitude modulation/amplitude modulation (AM/AM) and amplitude modulation/phase modulation (AM/PM) response (Fig. 3.2).

To avoid such undesirable nonlinear effects, a waveform with a high peak must be transmitted in the linear range of the HPA by decreasing the average power of the input signal. This is called input back-off (IBO) and results in a proportional output back-off (OBO) after the amplification. However, high back-offs reduce the power efficiency of the amplifier and cause a reduction in the coverage range. The operating point of the nonlinearity is defined by the input back-off (IBO) that corresponds to the ratio between the saturated and the average input powers:

$$IBO = 10log\frac{P_{in\ sat}}{E\{P_{in}\}} \tag{3.1}$$

where $P_{in\ sat}$ is the saturation power and $E\{P_{in}\}$ is the average input power. The amount of back-off is usually greater or equal to the PAR of the signal. Therefore, the power efficiency of an HPA can be increased by reducing the PAR of the transmitted signals. Hence, it is desirable to have signals which have the average and the peaks values as closer as together.

Finally, such high PAR leads to severe constraints on the dynamic range of the line drivers, as well as on the number of bits employed within the Analog-to-Digital Converter (ADC) and the Digital-to-Analog Converter (DAC). Therefore, high resolution linear CODECs (COder/DECoder) are required in order to achieve the desired quantization Signal-to-Noise Ratio (SNR), thus resulting in a greater complexity in the transmitter and the receiver.
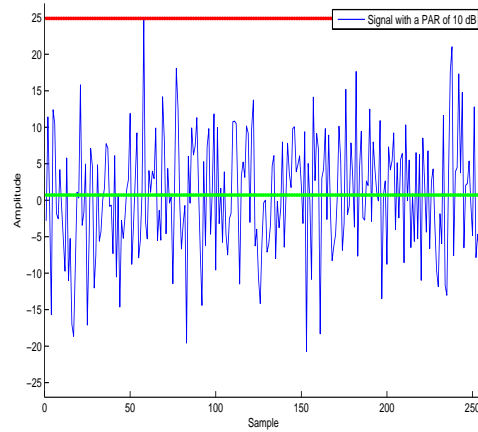
Figure 3.1: Time-domain OFDM signal with a peak-to-average ratio power of 10 dB. The OFDM signal has 128 subcarriers. The green line is the average of the signal and the red line is the highest peak.
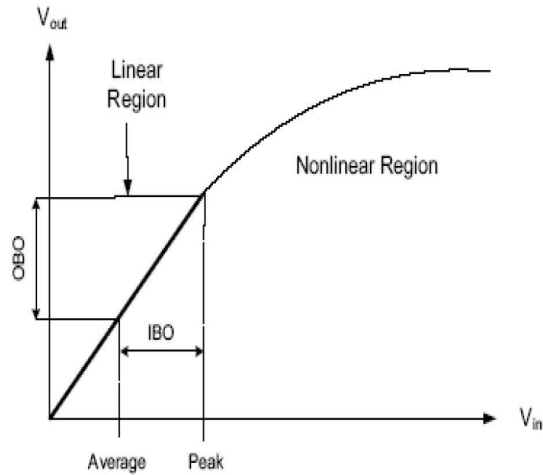
Figure 3.2: Typical power amplifier response.
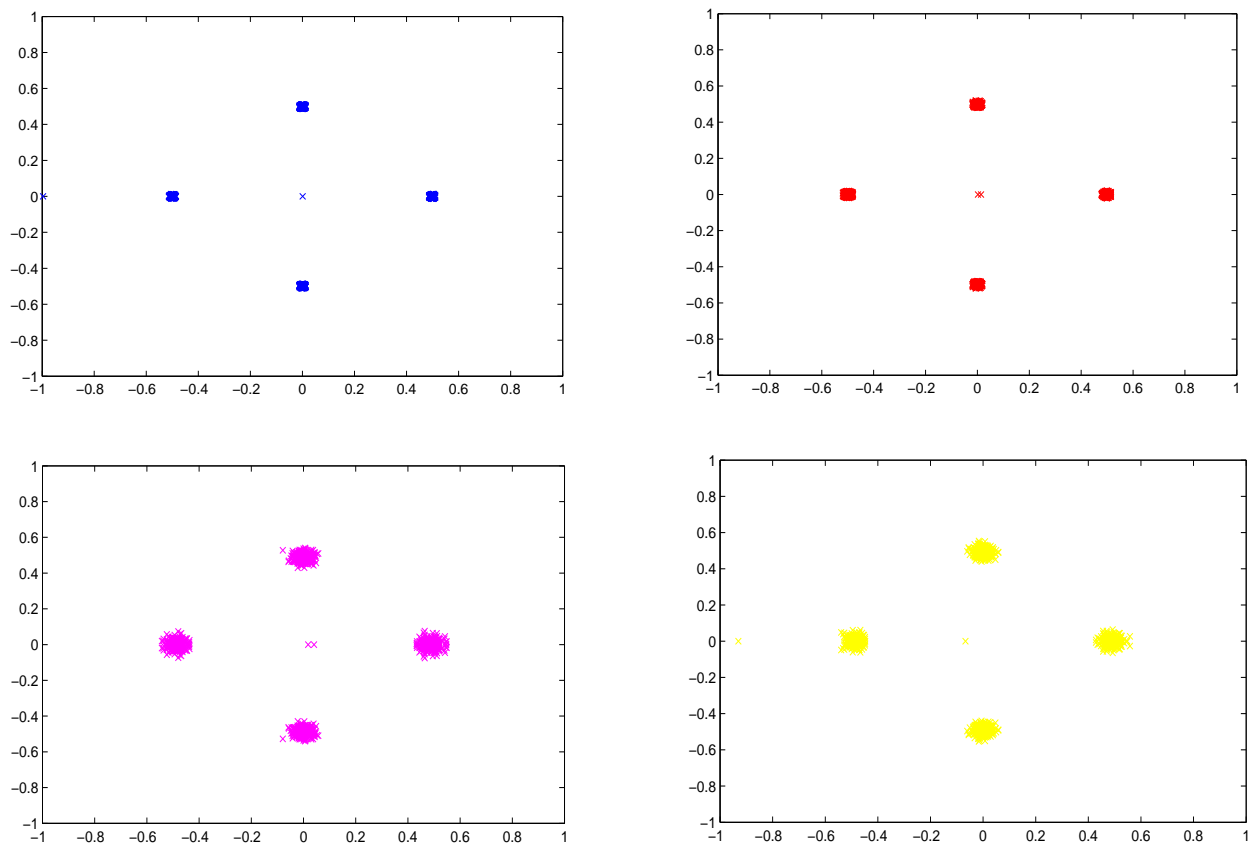
Figure 3.3: In-band distortion in a OFDM signal with a QPSK symbols caused by the nonlinearities of HPA. In the pictures are applied 1, 2 ,3 and 4 dB of clipping from top right to bottom left.

3.2   Problem Statement

In this section, the PAR problem is mathematically formulated and analyzed for the most common values of an OFDM signal. It also presents the tools to analyze statistically the PAR's improvement of the signal processing techniques which will be introduced in the following sections.

A multicarrier signal is the sum of many independent signals modulated onto subcarriers of equal bandwidth. In the case of OFDM, these carriers are orthogonal and with constant inter carrier spacing $\triangle f = 1/T$, where T is the OFDM symbol duration. The complex baseband representation of a multicarrier signal consisting of K subcarriers is given by

$$x(t) = \sum_{k=0}^{K-1} d_k e^{j2\pi k \Delta f t}, t \in [0, T] \tag{3.2}$$

The PAR is defined as the ratio between the maximal power and the average power,

$$PAR = \frac{\max_{0 \leq t < T} |x(t)|^2}{\frac{1}{T} \int_0^T |x(t)|^2 dt} \tag{3.3}$$

Since the signal is generated digitally, the PAR can be computed using discrete-time values $x_l = x(lT_s)$, $l = 0, \ldots N_s$. To accurately account for all the amplitude values, it is necessary to oversample the signal. An oversampling factor $L = N_s/K = 4$ is considered to be sufficient, since the error due to sampling can be bounded by [17]

$$|\max_t |x(t)| - \max_l |x_l|| \leq K[\cos^{-1}(\pi/2L) - 1] \tag{3.4}$$

Hence, the difference computing the PAR in a discrete signal can be as high as 1 dB, when the Nyquist rate is used. When L=4, the difference is negligible [18]. The PAR computed using a discrete oversampled signal is given by:

$$PAR = \frac{\max_{0 \leq k \leq N_s L - 1} |x_k|^2}{E\lfloor |x_k|^2 \rfloor} \tag{3.5}$$

3.2.1   Maximum expected PAR from an OFDM signal

From the previous section, it is shown that an OFDM signal is the sum of multiple sinusoidals having frequency separation $1/T$ where each sinusoidal gets modulated by independent information . Mathematically, the transmit signal is

$$x(t) = \frac{1}{\sqrt{K}} \sum_{k=0}^{K-1} d_k \cdot e^{j2\pi k \Delta f t}, \qquad 0 \leq t < KT_s. \tag{3.6}$$

For simplicity, let us assume in this section $d_k = 1$ for all the subcarriers. In that scenario, the maximum peak value expected is,

$$
\begin{aligned}
\max[x(t)x^*(t)] &= \max[\sum_{k=0}^{K-1} d_k \cdot e^{j2\pi k \Delta f t} \sum_{k=0}^{K-1} d_k^* \cdot e^{-j2\pi k \Delta f t}] \\
&= \max[d_k d_k^* \sum_{k=0}^{K-1} e^{j2\pi k \Delta f t} \sum_{k=0}^{K-1} e^{-j2\pi k \Delta f t}] \\
&= K^2
\end{aligned}
\tag{3.7}
$$

The mean square value of this signal is,

$$
\begin{aligned}
E[x(t)x^*(t)] &= E[\sum_{k=0}^{K-1} d_k \cdot e^{j2\pi k\Delta ft} \sum_{k=0}^{K-1} d_k^* \cdot e^{-j2\pi k\Delta ft}] \\
&= E[d_k d_k^* \sum_{k=0}^{K-1} e^{j2\pi k\Delta ft} \sum_{k=0}^{K-1} e^{-j2\pi k\Delta ft}] \\
&= K
\end{aligned}
\tag{3.8}
$$

Given so, the maximum Peak-to-Average Ratio for an OFDM system with K subcarriers and all subcarriers given the same modulation is

$$
PAR = \frac{K^2}{K} = K
\tag{3.9}
$$

This value corresponds to the value when all the subcarriers are equally modulated, so all the subcarriers align in phase and the peak value hits the maximum. Therefore, the maximum expected value increases with the number of subcarriers, K. This characteristic is shown in Fig. 3.4.

3.2.2 Statistical analysis

Since an OFDM signal is a random process, its PAR is commonly characterized by the complementary cumulative distribution function (CCDF). The CCDF is defined as the probability that PAR exceeds a certain threshold, $\Pr(PAR > PAR_0)$. When a large number of carriers is used, an OFDM signal can be modeled as a complex Gaussian random process, instantaneous power (square of the amplitude) thus follows a central chi-square distribution with two degrees of freedom [19]. Fig. 3.4 shows an example of the so-obtained CCDF of the PAR.

The CCDFs are usually compared in a graph such as Fig.3.4, which shows the CCDFs of the PAR of an OFDM signal with 64, 128, 256 and 512 subcarriers for quaternary phase shift keying modulation (QPSK).
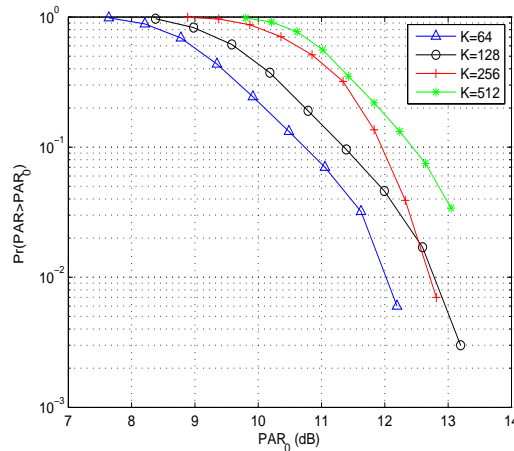
Figure 3.4: CCDF of the PAR for a QPSK OFDM signal with varying number of carriers.

Another common measure to evaluate PAR techniques is the Signal to Distortion Ratio (SDR) which is defined as:

$$
SDR = \frac{\| x(t) \|^2}{\| x(t) - g(x(t)) \|^2}
\tag{3.10}
$$

where $g()$ is the function that represents the non-linearity caused by the high peaks. If the nonlinearity g() is the clipping effect encountered in the soft limiters, then the amplifier response is modeled as

$$\bar{\tilde{x}}(t) = g_1[\tilde{x}(t)] = \begin{cases} \tilde{x}(t), & |\tilde{x}(t)| \le A \\ A, & \tilde{x}(t) > A \\ -A, & \tilde{x}(t) < -A \end{cases} \qquad (3.11)$$

On the other hand, for the hard limiter model, this function is given by [20]

$$\bar{x}(t) = g_2[x(t)] = \begin{cases} x(t), & |x(t)| \le A \\ \frac{4}{\pi} A e^{j \arg[x(t)]}, & |x(t)| > A \end{cases} \qquad (3.12)$$

3.3 Overview of existing techniques

The present section focuses on the existing and well-known PAR reduction techniques for multicarrier transmission and examples of the same.

3.3.1 Clipping and filtering

Introduction

The simplest technique of PAR reduction is amplitude clipping [2,3]. It limits the peak envelope of the input signal to a predeterminate value, or otherwise passes the input signal unperturbed, that is

$$
y[x] = \begin{cases} x & if\,|x| \le A \\ A \cdot e^{jarg(x)} & if\,|x| > A \end{cases}
\tag{3.13}
$$

Fig. 3.5 shows the block diagram of a possible implementation. The input signal symbols $\mathbf{A}_i$ are transformed using an oversized inverse fast Fourier Transform (IFFT) which reproduces the effect of oversampling. For an oversampling rate of L, A_i is extended by adding $K(L-1)$ zeros.

Subsequently, this oversampled signal is clipped. Hard limiting model is assumed when the signal amplitude is clipped, but any other form of non-linearity can be used. Due to clipping, there is a distortion in the signal. The distortion can be seen as another source of noise. This noise is both out-band and in-band. Therefore, the clipping is followed by filtration to reduce out-of-band power.

The filtration process consists of two FFT operations. The forward FFT transforms the clipped signal back into discrete frequency domain resulting in vector $\mathbf{C}_i$. The in-band discrete frequency components $c_{0,i}, ..., c_{K/2-1,i}, ..., c_{KL-1,i}$ are passed unchanged to the inputs of the second IFFT while the out-band components are discarded.

Although filtration after clipping is required to reduce the out-of-band clipping noise, different filtrations can be applied. For instance, in the paper [2] an equiripple bandpass finite-impulse response (FIR) filter with 103 coefficients is used. The stopband attenuation is designed to be 40 dB to guarantee a very low interference level to the neighboring OFDM channels. The passband ripple is 1 dB.
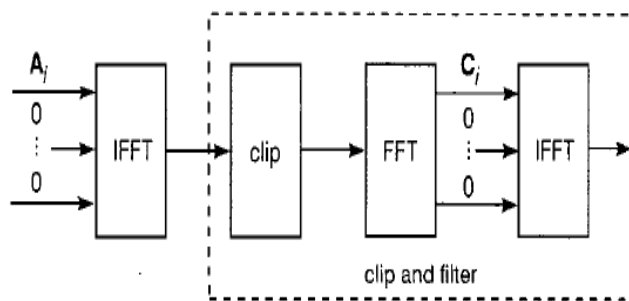
Figure 3.5: Block diagram of clipping and filtering PAR reduction technique.

The performance of this technique is not limited by out-of-band noise , otherwise is constraint by the in-band distortion caused by the clipping noise. Hence, the in-band distortion will determine the maximum achievable PAR reduction.

Several authors have been studying the effect of nonlinearities in OFDM symbols [21]. Bussang's theory assumes that real and imaginary parts have Gaussian statistics. The theory also develops a model given by the following expression

$$y(t) = \alpha x(t) + d(t) \tag{3.14}$$

where $x(t)$ is the input of the nonlinearity, α is a constant and $y(t)$ is the output. $d(t)$ is a zero mean random noise process which is uncorrelated with $x(t)$. Finally the constant α is determined by

$$\alpha = \frac{E\{y(t)x^*(t)\}}{E\{x(t)x^*(t)\}} \tag{3.15}$$

This theory is applied to compute the nonlinearity during the clipping and filtering process. Although this theory only applies in the first stage of clipping and filtering, it is employed by ignoring the second order errors in the analysis. In the absence of distortion and noise in the channel, samples of sections of $y(t)$ are input to the receiver FFT. Thus the vector output from the FFT for the ith received symbol can be described by

$$\mathbf{Z} = \alpha \mathbf{A}_i, + \mathbf{B}_i \tag{3.16}$$

where $\mathbf{B}_i$ is the FFT of the vector of samples of $d(t)$. Therefore, the Signal and Clipping Noise Ratio (SCNR) in the kth subcarrier can be computed by:

$$SCNR_k = \frac{\alpha^2 E\{|a_{i,k}|^2\}}{E\{|b_{i,k}|^2\}} \tag{3.17}$$

where $a_{i,k}$ and $b_{i,k}$ are the ith element of the matrix A_i and B_i, respectively. As a result, the SCNR value depends on the subcarrier.

Results and performance

First of all, we focus on the spectral splatter caused by clipping and the effect of filtering. The Power Spectral Density (PSD) is measured for each OFDM block and then averaged over many blocks to eliminate the effects of the rectangular time window. In Fig. 3.6, the PSD of the clipped signal with various CR from 0.8 to 1.6 is shown. The in-band signal attenuation as well as the out-of-band caused by clipping is evident. For CR= 1.4 , the out-of-band noise emission power is only 16 dB lower than the signal power. This shows that filtering is necessary to suppress the spectral splatter caused by clipping.

Then, Fig. 3.7 shows the SCNR value for different Clipping Ratio (CR) values. Clipping Ratio (CR) is defined as the ratio between the clipping value and the root mean square value (rms) of the signal ($C = A/\sigma$). It is easy to show that, for an OFDM signal with N subchannels $\sigma = \sqrt{N}$ for a baseband signal and $\sigma = \sqrt{N/2}$ for a bandpass signal. In the case of bandpass signal with $N = 128$ subcarriers $\sigma = 8$. A CR of 1.4 means the clipping level is about 3 dB higher than the rms level.

Results show that even for severe clipping, the SCNR is quite large. This is because the main effect of clipping is to reduce the value of α rather than increase the variance of $b_{i,k}$.

Clipping causes in-band noise, which causes a degradation in the BER performance. Fig. 3.8 shows the BER performance as a function of the received signal-to-noise ratio (SNR), averaged across all the subchannels, with clipping and filtering over a channel of additive white Gaussian noise. For hard clipping (CR = 0.8) , the degradation is more than 4 dB at the 10^{-2} BER level. But when CR$\geq$ 1.4, less than 1 dB penalty is encountered.

Conclusion

The PAR of an OFDM signal can be reduced without any increase in out-of-band power by clipping the oversampled time domain signal followed by filtration. An example of an easy implementation of filtration is using the FFT and discarding the out-of-band values. Filtering produces peak regrowth and clipping produces an in-band distortion that can be seen as noise-like effect.

Finally, the performance of this technique is constraint by the maximum tolerated in-band distortion in our system which is caused by the clipping noise. The clipping noise is added in the transmitter rather than the receiver. Hence, in fading channels, the noise introduced by clipping is less than the noise introduced by the channel since the clipping noise fades along with the signal.
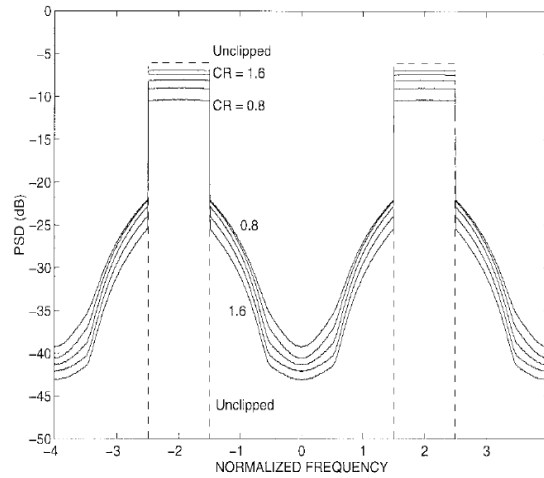
Figure 3.6: Power spectral density of the unclipped and clipped OFDM signals [2].
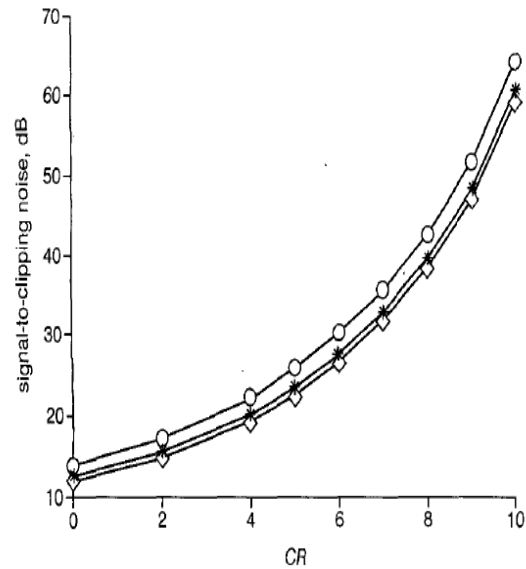
Figure 3.7: Signal-to-clipping noise ratio for K=128, an oversampling rate L=2 and 5000 OFDM symbols simulated [3].
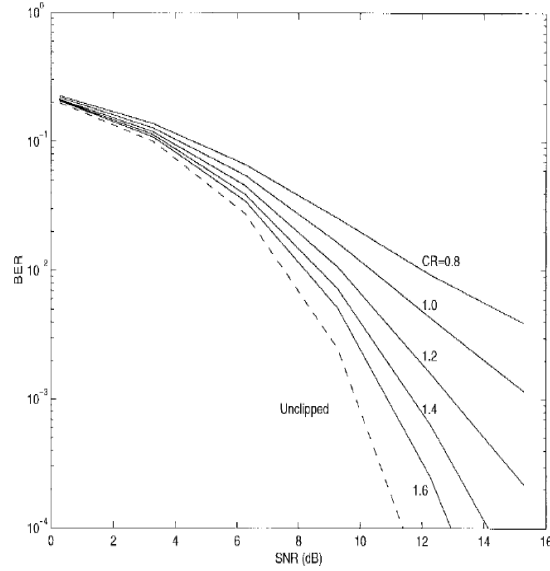
Figure 3.8: BER of the clipped-and-filtered OFDM signals as a function of the CR [2].

Data Block	PAR (dB)	Data Block	PAR (dB)
1,1,1,1	6.4	1,1,1,-1	2.33
1,1,-1,1	2.08	1,-1,1,1	2.33
-1,1,1,1	2.08	1,1,-1,-1	3.63
1,-1,-1,1	2.3	-1,-1,1,1	3.6
-1,1,1,-1	3.63	1,-1,1,-1	6.4
-1,1,-1,1	6.4	-1,1,-1,-1	3.63
-1,-1,1,-1	2.08	-1,-1,-1,1	2.33
1,-1,-1,-1	2.08	-1,-1,-1,-1	6.4

Table 3.1: Example codification technique

3.3.2   Coding technique

Introduction

Coding can also be used to reduce the PAR of an OFDM symbol. The simple idea consists in selecting those codewords which provide a reduced PAR value for transmission [22]. This idea is illustrated in the following example.

   Example. The PAR values of all possible combinations of an OFDM symbol with 4 subcarriers and a BPSK modulation are computed and memorized as it is represented in Table 3.3.2. It can be seen from this table that four blocks result in PAR of 6.4 dB, on the other hand, seven blocks result in a PAR of 2.08 dB. It is clear that we could reduce PAR by avoiding transmitting those sequences. Based on these results, it can be done by block coding which data such the 3-bit data word is mapped onto 4-bit codeword such that the set of permissible sequences does not contain sequences which have large PAR.

   However, this approach requires an exhaustive search to find the best codes and to store in a large look-up table for encoding and decoding. Furthermore, there is a data rate loss caused by coding and this approach does not address the error correction that is expected from coding. A more complex idea is presented in [23] which consists in using codewords drawn from offsets from a linear code. The idea consists in choosing the codewords which minimize the PAR and offer an error correction.

Event	Probability	Huffman code
A	0.154	1
B	0.110	01
C	0.072	0010
D	0.063	0011
E	0.059	0001
F	0.015	000010
G	0.011	000011

Table 3.2: Example Encoding Table

Impact of Huffman codes in PAR

There are studies which show the Huffman codification is beneficial for PAR reduction [4]. The Huffman method was developed in the 1950s by D.A. Huffman. The idea is to assign frequently used signal sample values fewer bits, and seldom used sample values more bits to make an appropriate compression for the signal to be transmitted. In mathematical terms, the optimal situation is reached when the number of bits used for each sample is proportional to the logarithm of the sample's probability of occurrence, as it is shown in table 3.3.2.

The Huffman encoding causes the PAR reduction, that is because encoding produces frequently occurring symbols are assigned a lower number of bits rather than the less probable to occur symbols, and thus when rearranging the stream of bits among symbols with fixed number of bits , the probability of repeating the same symbol will be eliminated, preventing the coherent addition of the multicarrier signals that cause the undesired high peak. Fig. 3.9 shows the PAR improvement when Huffman is applied in the transmission.
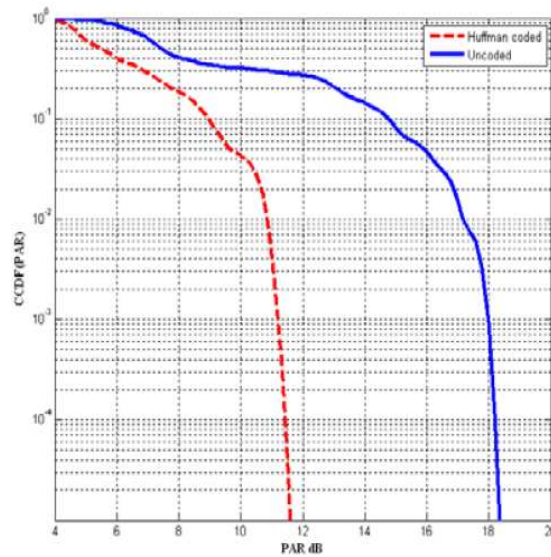
Figure 3.9: CCDF with/without Huffman encoding in an OFDM signal with 16-QAM modulated, N=256 subcarriers and L = 2 [4].

Conclusion

Due to the need of an exhaustive search through the codewords and the need of storing large look-up tables, the technique reduces the usefulness of codification techniques for multicarrier systems with a small number of subcarriers. On the other hand, Huffman codes provide a significant reduction in the PAR, thus reducing

the nonlinearities caused by power amplifiers.

3.3.3 The partial transmit sequence technique

Introduction

The Partial Transmit Sequence (PTS) technique is a distortionless scheme for PAR reduction in OFDM symbols [5, 24]. The main idea is based in the coordination of proper phase rotation signal parts to minimize the peak power of a multicarrier signal.

In order to implement this idea, the input data block of K symbols is partitioned into M pairwise disjoint blocks X_k, $k = 1, ..., M$ (See Fig 3.10). Mainly, the total number of subcarriers included in any one of these subblocks X_k is arbitrary, but subblocks of equal size have been found to be an appropriate choice [24]. All subcarrier positions in X_k, which are already represented in another subblock, are initialized to zero, so that $X = \sum_{k=1}^{M} X_k$.

Each subblock is weighted by a set of rotation factors $b_k(u)$ where $u = 1..U$, so that a modified subcarrier vector $\widetilde{X} = \sum_{k=1}^{M} X_k \cdot b_k(u)$ is obtained, which represents the same information as X, if the set $b_k(u)$ is known for each u and k. The phase factors are selected such that the PAR of the combined signal is minimized (Fig. 3.10).
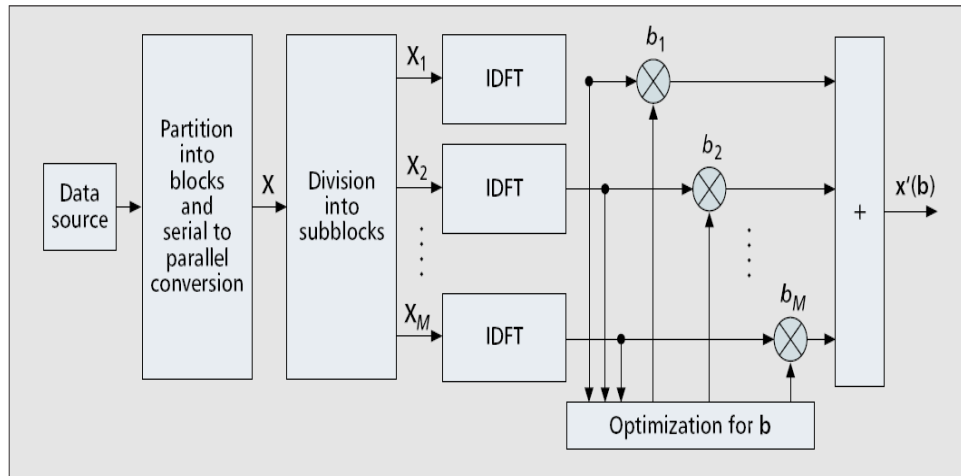
Figure 3.10: Block diagram of the PTS technique.

Mathematically, it is expressed as:

$$\{b_1(u), b_2(u), ..., b_M(u)\} = argmin_u \left(max_{0 \leq n < N_s L - 1} \left| \sum_{k=1}^{M} IDFT(X_k) \cdot b_k(u) \right| \right) \tag{3.18}$$

where $b_k(u) = e^{j\phi(u_k)}$, $\phi(u_k) \in [0, 2\pi)$. Resulting in the optimum transmit sequence

$$\tilde{x}(u_{opt}) = \sum_{k=1}^{M} IDFT(X_k) \cdot b_k(u_{opt}) \tag{3.19}$$

where u_{opt} is the phase vector that gives the greater reduction.

Hence, $U^{(M-1)}$ is the amount of sets of phase factors that are evaluated to find the best case. The total complexity increases exponentially with the number of subblocks M. The receiver needs to know the set
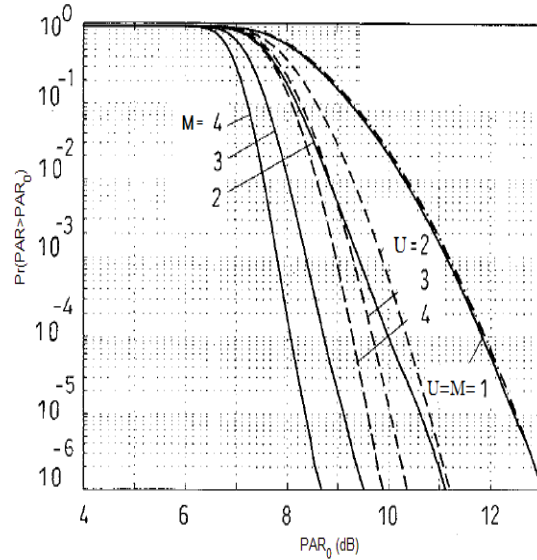
Figure 3.11: CCDF PAR of OFDM signal with 512 subcarriers which has been applied the PTS and SLM techniques with different values of V and M. The dashed lines correspond to SLM technique, whereas the straight lines corresponds to the PTS technique [5].

$b_k(u)$. Hence, an unambiguous representation of it must be transmitted to the receiver. As a consequence, the amount of bits as side information is $\lfloor log_2 U^{(M-1)} \rfloor$.

As mentioned above, the ordinary PTS technique has exponentially increasing search complexity. To reduce the search complexity, various techniques have been suggested. In [25], iterations for updating the set of phase factors are stopped once the PAR drops below a preset threshold.

This technique is summarized in the following example: an OFDM system has six subcarriers that are divided into three blocks with the same amount of information, $X_1 = [1, -1, 0, 0, 0, 0]$, $X_2 = [0, 0, 1, 1, 0, 0]$, $X_3 = [0, 0, 0, 0, -1, -1]$. The set of phases used to minimize the PAR value is $b_k(u_k) = \pm 1$. The original data, which is the sum of X_k, has a PAR of 10.2 dB. There are 2^{3-1} ways of combining subblocks without counting the original subblock. Among them, $[b_1, b_2, b_3] = [-1, 1, -1]$ achieves the lowest PAR value which is 7.2 dB. Therefore, it provides a reduction of 3 dB. The amount of side information is 3 bits.

Results and performance

Fig. 3.11 presents simulation results obtained from PTS with $b_k(u) \in \{\pm 1, \pm i\}$ and a block partitioning with subblocks of exclusively adjacent subcarriers and an equal number of subcarriers in them. M = 1 corresponds to the original OFDM.. Note that PTS OFDM with M = 4 blocks and therefore three free rotation factors and four allowed angles for each, corresponds to a redundancy of 6 bits on 512 carriers. If QPSK in the subcarriers and some inactive (zero) carriers are assumed, this is well below 1 % redundancy to achieve a crest factor reduction of significant 4 dB at probability of 10^{-5}. For comparison, results for SLM-OFDM are included with U = 2, ..., four alternative transmit signals. It is obvious that PTS performs better than SLM, if we consider the same number of IDFTs (U = M), required to generate one favorable OFDM symbol.

Conclusion

PTS offers an efficient and distortionless scheme for peak power reduction. However, it introduces some additional complexity in the receiver and side information, thus reducing the data rate of the transmission.
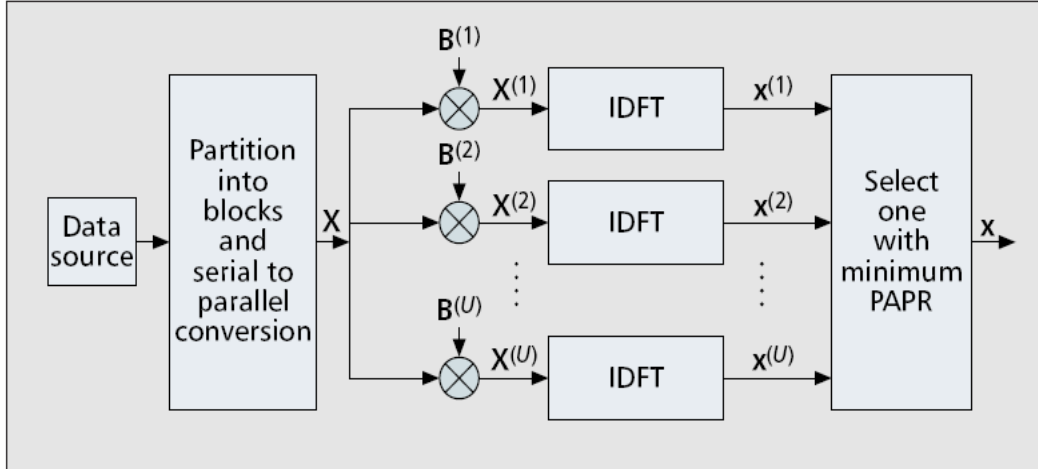
Figure 3.12: Block diagram of the SLM technique.

The approach is very flexible and works with an arbitrary number of subcarriers and without restriction in the applied modulation.

3.3.4 Selected Mapping Technique

Introduction

The Selected Mapping Technique consists of adding a set of phases in the transmitted signal in order to avoid phase alignment [26]. This idea is similar to the PTS technique. However, in SLM technique, the transmitter generates a set of sufficiently different candidate data blocks, all of them representing the same information. Subsequently, the most favorable is selected for transmission.

To implement this idea each data block is multiplied by U different phase sequences, each of length K in order to modify the original data:

$$x\left(t\right)^{(u)} = \frac{1}{\sqrt{K}} \sum_{k=0}^{K-1} d_k \cdot b_k^{(u)} e^{j2\pi k \Delta f t} \tag{3.20}$$

where $0 \leq t < KT_s$, $\mathbf{B}^{(u)} = [b_0^{(u)}, b_1^{(u)}, ..., b_{K-1}^{(u)}]$ with $b_k^{(u)} = e^{j\varphi_k^{(u)}}$, $\varphi_k^{(u)} \in [0, 2\pi)$ and $u = 1, ..., U$. Among the U modified data blocks, $x\left(t\right)^{(u)}$, the one with the lowest PAR is selected for transmission (Fig. 3.12).

Information about the selected phase sequence should be transmitted to the receiver as side information. At the receiver, the reverse operation is performed to recover the original data block. For implementation, the SLM technique needs U IFFT operations, and the number of required side information bits is $\lfloor log2U \rfloor$ for each data block.

The following example summarizes the SLM technique: an OFDM system has six subcarriers. We set the number of phase sequences to $U = 4$ (2 bits of side information). The data block to be transmitted is denoted $X = [1, 1, 1, 1, -1, -1]^T$ whose PAR before applying SLM is 6 dB. We set the four phases as $B(1) = [1, 1, 1, 1, 1, 1]^T$, $B(2) = [-1, -1, 1, 1, 1, -1]^T$, $B(3) = [-1, 1, -1, 1, -1, 1]^T$, $B(4) = [1, 1, -1, 1, -1, 1]^T$. Among the four modified data blocks $X(u)$, $u = 1, 2, 3, 4$, $X(2)$, has the lowest PAR of 4.0 dB. Hence, $X(2)$ is selected and transmitted to the receiver. For this data block, the PAR is reduced from 6 to 4 dB, resulting in a 2 dB reduction. The amount of PAR reduction may vary from data block to data block. The design of the set phases and the amount of set phases determine the PAR reduction.

Results and performance

A 512 carrier OFDM system with QPSK modulation was simulated and 10^3 OFDM symbols were generated. For the use of symbol interleaving, the 512 OFDM QPSK symbols were multiplied by different number of phase vectors ($U= 2^1$, 2^2 and 2^3). For the case of $U=2$, at the probability of 10^{-2}, the PAR is reduced approximately 1.5 dB. For the case of $U=8$, the PAR is reduced 2.5 dB at the probability of $2 * 10^{-2}$ as it is shown in Fig. 3.13. The amount of PAR reduction for SLM depends on the number of phase sequences U (See Fig. 3.13) and the design of the phase sequences. Therefore, there is a trade-off between the data rate loss and the PAR reduction capability.
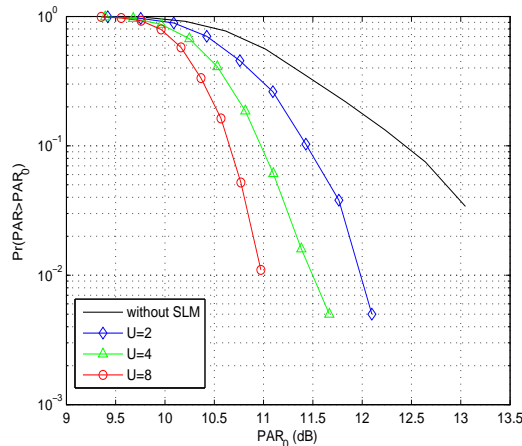
Figure 3.13: CCDF PAR of an OFDM signal of 512 subcarriers and using the SLM technique varying the amount of required side information.

Conclusions

The proposed scheme for the reduction of PAR can be used for arbitrary numbers of carriers and any signal constellation. Selected mapping provides significant gains at moderate additional complexity. Actually, it is appropriate for all kinds of multiplex techniques, which transform data symbols of the transmitted signal. However, the index of the selected phase has to be transmitted to the receiver in order to decode the signal. It also produces a reduction in the data rate.

SLM and PTS are similar techniques with similar characteristics. SLM also offers an efficient and distortionless scheme by increasing complexity in the transmitter and receiver and reducing the data rate. Both techniques are flexible with the modulation and the number of subcarriers.

The main differences between them are: SLM is better than PTS in terms of reduction capability vs redundancy, but PTS is considerably better with respect to reduction capability vs. additional complexity in the systems (e.g. number of IDFTs) as it is capable of provide more reduction. Obviously, complexity is the main factor, if practical OFDM systems are considered and so PTS (in an efficient implementable structure) could be a strong candidate.

PTS and SLM are near-optimum when PAR reduction capability vs. redundancy is considered. Thus, they seem to be the most powerful and flexible methods known to reduce OFDM peak power without nonlinear distortion.
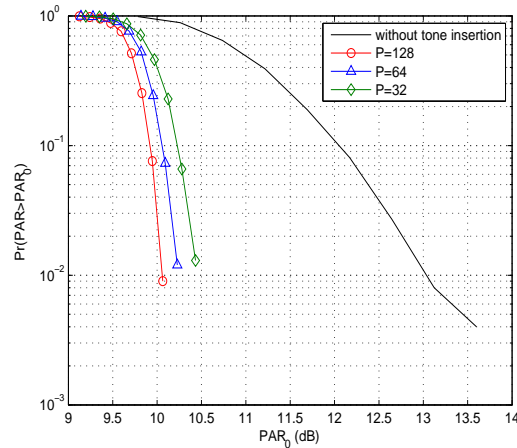
Figure 3.14: CCDF of OFDM signal with P-1 interleavers.

3.3.5   Interleaving technique

Introduction

The interleaving technique is grounded on the heuristic notion that highly correlated data frames have large PARs, which could thus be reduced, if the long correlation patterns were broken down. We therefore employ P-1 interleavers, each of which produces a re-ordering or permutation of the K symbols of the input data frame [9, 27].

An interleaver is a device that operates on a block of K symbols and reorders or permutes them; thus, data block $X = [X_0, X_1, ..., X_{K-1}]^T$ becomes $X = [X_{(0)}, X_{(1)}, ..., X_{(K-1)}]^T$ where $\{n\} \leftrightarrow \{\pi(n)\}$ is a one-to-one mapping $\pi(n) \in \{0, 1, ..., K-1\}$ for all K symbols. The permutation with the lowest PAR of all the P frames (P-1 permutations and the original) is selected for transmission.

However, to recover the original data block it is also necessary to transmit the permutation index to the receiver; thus the number of bits required for side information is $\lfloor log_2(P) \rfloor$. Furthermore, both transmitter and receiver store the permutation indices $\pi(n)$ in memory.

Results

A 512 carrier OFDM system with QPSK modulation was simulated and 10^4 OFDM symbols were generated. For the use of symbol interleaving,the 512 OFDM QPSK symbols of a frame were permuted by different interleavers. For P=32, the 1 % is reduced by 2.6 dB. In the case of P=128, the 1 % by 3 dB. As it was expected, there is a compromise between the number of interleavers and the improvement. Hence, there is a tradeoff between the required side information and the improvement achieved.

Conclusions

For this technique, P-1 random interleavers are used to produce P-1 permuted sequences from the same information. A compromise between the number of possible permutations and the PAR reduction is noted in the results.

However, the worst case of PAR, that is a value of K, is extremely unlikely for random data. Since the Interleaving approach does not attempt to reduce the worst case, the data rate loss of this method is negligible. The method is of similar complexity to the PTS method, and achieves comparable results. Notably, the Interleaving approach can also be used in conjunction with other methods such as PTS or SLM.

3.3.6 Active Constellation technique

Introduction

Active Constellation (ACE) uses nonbijective constellation to reduce the PAR by appropriately encoding the data symbols [6,7]. The idea is easily explained in the case of flat-power OFDM with Quadrature Phase Shift Keying (QPSK) modulation. For an individual channel, there are four possible constellation points, which lie in each quadrant in the complex plane and are equidistant from the real and imaginary axes. Assuming white Gaussian noise, the maximum-likelihood decision regions are the four quadrants bounded by the axes, and thus a received data symbol is assigned according to the quadrant in which the symbol is observed.

Errors occur when noise translates the received sample into one of the other three quadrants. Any point that is farther from the decision boundaries than the original constellation point (in the proper quadrant) will offer increased margin, which guarantees a lower error rate. Therefore, it allows the modification of constellation points within the quarter-plane outside of the nominal constellation point with no degradation in performance. The extended region is represented in Fig. 3.15.
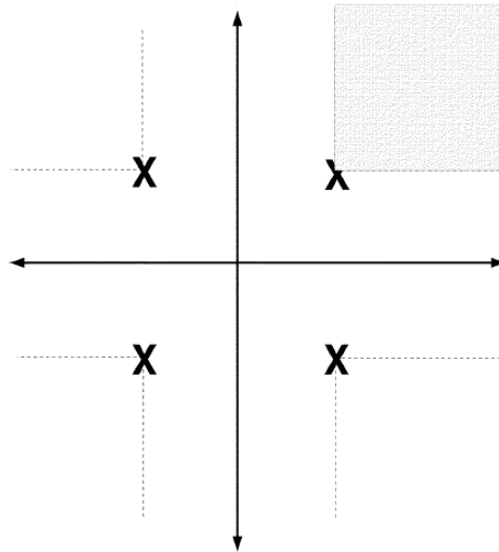
Figure 3.15: Depiction of active channel extension with QPSK encoding. The shaded region represents the extension region for the first-quadrant data symbol

The ACE idea can be applied to other constellations as well, such as QAM and M-PSK constellations, having points outside of the constellation allow an increase in margin without degrading the error probability in the transmission. However, the inside constellation points cannot be translated because it would decrease the BER. Therefore, constellations with more inside points offer less performance. This problem is also present in modulations with larger constellations because the extended region is smaller.

The effect in OFDM symbols is the increase of the amplitude which adds sinusoidal component in a certain subcarrier. If adjusted intelligently, a combination of these additional signals can be used to partially cancel time-domain peaks in the transmitted OFDM signal. However, the farther points (or higher amplitude) imply an increase in the total transmitted power. As a consequence, there is a tradeoff between added power and PAR reduction capability. This tradeoff will be analyzed soon in this section.

In order to analyze the ACE technique, the following concepts are defined:

- Relative constellation error (RCE) , ϵ , is defined as

$$\epsilon = \sqrt{\frac{\sum_{k=0}^{K-1}|d(k)-d_0(k)|^2}{KP_0}} \tag{3.21}$$

where $d(k)$ is the distorted or extended constellation and $d_0(k)$ is the original undistorted constellation at the kth subcarrier. P_0 is denoted as the average transmit power of the signal using the original constellation d_0. Therefore the energy given by the modified constellation is

$$\|d\|^2 = \|d_0\|^2 + \|d-d_0\|^2 + 2\Re\{d_0^*(d-d_0)\} \tag{3.22}$$

- The relative average power added due to the constellation modification is ρ . Note that ρ is quite different from ϵ :

$$\rho = \epsilon^2 + \frac{2\Re\{d_0^*(d-d_0)\}}{KP_0} \tag{3.23}$$

ACE problem minimization

In ACE there are specific constraints in regions where the constellation symbols can be modified in order to not increase the overall BER. This implies that only outer points can be modified for PAR reduction and the constellation points must be extended outward, so it implies that there is always an increase in power. However, the power has to be constraint to a maximum value, ρ_{max}. Our goal is to obtain the optimal constellation symbol vector d, which minimizes the PAR subject to the different constraints on the constellation. It can be express as:

$$\text{minimize} \qquad PAR \tag{3.24}$$

$$\text{subject to} \qquad \frac{\|d\|^2}{KP_0} \leq 1 + \rho_{max} \tag{3.25}$$

$$\text{d} \; \epsilon \; C \tag{3.26}$$

$$d(A) = d_0(A) \tag{3.27}$$

The set C denotes a convex set of allowed regions for d to be in. This set ensures that only the outer constellation points are modified. We use $d(A)$ to denote the vector of constellation symbols subcarrier indices defined by the set A respectively. The set A is the set of inside constellation points in the modulation. Hence, the third constraint specifies that the inside constellation points must remain equal.

The ACE is a convex problem whose solution is guaranteed to be the global minimum PAR solution given the above constraints [6]. Figure 3.16 shows a constellation symbols after solving the optimization problem for several OFDM symbols with the original constellation of 16-QAM and ρ_{max}= -10 dB.

In the literature [7], different techniques are presented to solve this problem efficiently: a projection onto convex sets approach, a gradient-project approach in which the best stepsizes that leads to very fast convergence toward a low-PAR solution are determined.

Performance evaluation

The ACE with a simple gradient algorithm was tested for a OFDM signal with subchannels employing 16-QAM using randomly generated OFDM symbols [6]. As it was stated before, the PAR reduction capacity in the ACE technique depends on the amount of power, ρ. Fig 3.17 depicts the PAR CCDF for 16-QAM for various values of ρ. It shows the tradeoff between the PAR and the consumed power ρ.

Results by implementing fast algorithms.   The ACE with a simple gradient algorithm was tested for an OFDM signal with subchannels employing QPSK using randomly generated OFDM symbols [7]. Simple Gradient Algorithm iterations were applied whenever the PAR of the symbol block was greater than 6 dB. Fig. 3.18 shows the digital PAR results of up to four iterations applied to the given system.
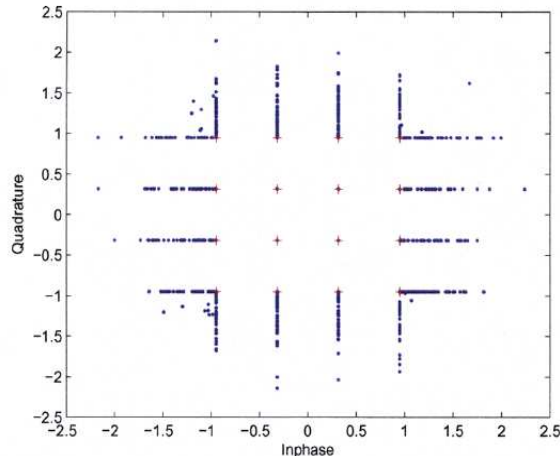
Figure 3.16: ACE for a 16-QAM constellation with ρ_{max}=-10 dB

The performance of the first iteration is fantastic, as a PAR reduction of up to 5 dB can be achieved. The second iteration provides only an additional half dB of reduction, while a third iteration produces an almost negligible reduction (except near symbol 10^{-3} clip probability). Further iterations provide negligible increase in performance.

The projection onto convex sets approach was simulated with the same clip parameters as above and the PAR results are shown in Fig. 3.19. Slow convergence in the ACE technique is observed. Simple Gradient approach is faster, thus making better algorithm for practical systems. [1]

Constellation Distortion (CD) problem minimization

A similar idea that ACE is called Constellation Distortion (CD) [28] technique. The idea of CD is to distort constellation symbols in order to reduce PAR. Adding distortion results in larger BER, but reduces PAR. In CD, the tradeoff is between PAR reduction and the added distortion.

The inputs to the CD minimization block are d_0, ϵ_{max} and A_D. We want to minimize the PAR subject to constraints on the maximum allowed relative constellation error (RCE), ϵ_{max}^2. It is desirable to formulate the problem as a convex problem in order to guarantee a global minimum. However, a lower bound on average power causes to be non-convex problem [7].The optimization problem is

$$\text{minimize} \qquad PAR = \frac{x(d)}{\|x\|} \tag{3.28}$$

$$\text{subject to} \qquad \frac{\|d-d_0\|^2}{KP_0} \leq \epsilon_{max}^2 \tag{3.29}$$

$$\Re\{d_0^*(d - d_0)\} \geq -\epsilon_{max}^2/2 \tag{3.30}$$

$$d(A) = d_0(A) \tag{3.31}$$

where $d(A)$ denotes the vector constellation symbols indices that are referred by the set A. The third constraint specifies that only the data subcarriers are to be distorted. Figure 3.20 shows a constellation after solving the optimization problem for several OFDM symbols with original constellation of 16-QAM and ρ_{max}= -10 dB.

---

[1]I recommend the lecture of [7] for further information about how to implement these fast convergence algorithms.
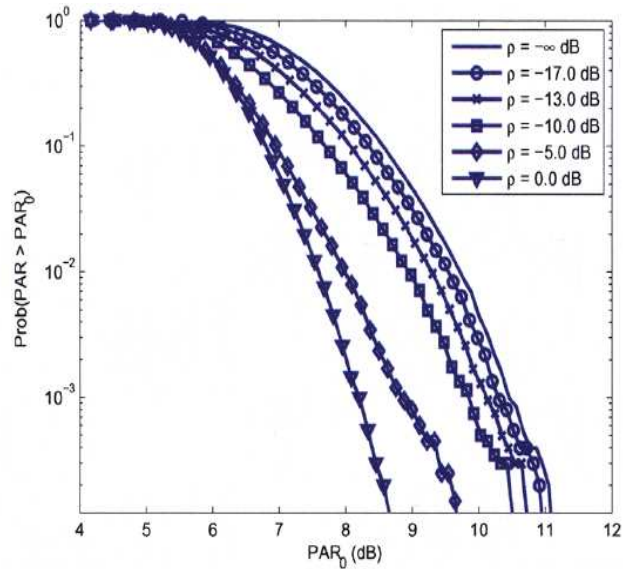
Figure 3.17: PAR CCDF of 16-QAM OFDM using ACE and as a function of ρ [6].
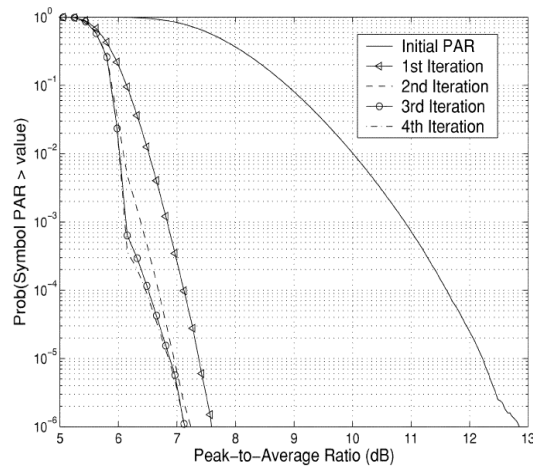
Figure 3.18: PAR results of ACE-SGP method applied to an OFDM system with 256 subchannels employing QPSK [7].

As it was stated before, the PAR reduction capacity in the ACE technique depends on the relative constellation error , ϵ. Fig 3.21 depicts the PAR CCDF for 16-QAM for various values of ϵ_{max}. It shows the tradeoff between the PAR and maximum allowed distortion in the CD technique.

Conclusions

The ACE technique presents a scheme that simultaneously slightly decreases the BER while substantially reducing the Peak-to-Average Ratio. Furthermore, there is no loss in data rate and no side information is required. However, these modifications increase the transmitted power for the data block, and the usefulness of this scheme is rather restricted to a modulation with a large constellation size.

The CD technique is presented as a contrast with the ACE technique. The CD technique distorts the constellation without increasing power, while the ACE extends the constellation by adding power. The results for the CD technique illustrate that the tradeoff is between PAR reduction and added distortion, which
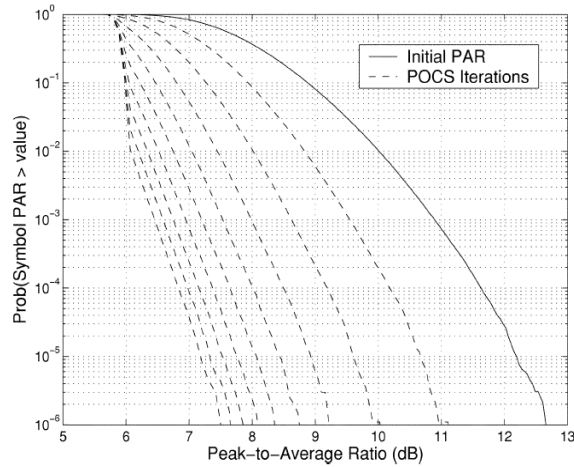
Figure 3.19: PAR results of ACE-POCS method applied to an OFDM system with 256 subchannels employing QPSK [7].

results in a larger BER. For the ACE approach, results show that the tradeoff is between the added power and the PAR reduction.

3.3.7 Tone Reservation

Introduction

The Tone reservation (TR) technique is based on adding a data-block-dependent time domain signal to the original multicarrier signal to reduce its peaks [8, 29]. This time domain signal is computed to mitigate the large peaks in the block signal.

Generally, TR exploits unused (due to low SNRs) or reserved tones to introduce a peak-canceling signal that can reduce the peak power of a transmitted data block. Since these reserved subchannels are orthogonal, this additive signal causes no distortion of the data-bearing subchannels. Obviously, these tones will sacrifice capacity, but our goal is to keep this capacity loss small, while achieving valuable PAR reduction. In the
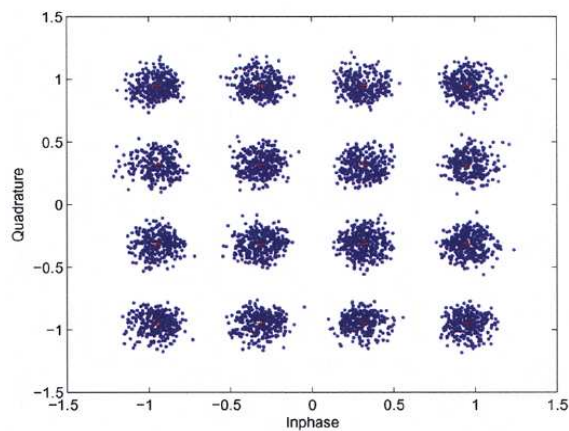
Figure 3.20: CD for a 16-QAM constellation with ϵ_{max}=-19 dB [6].
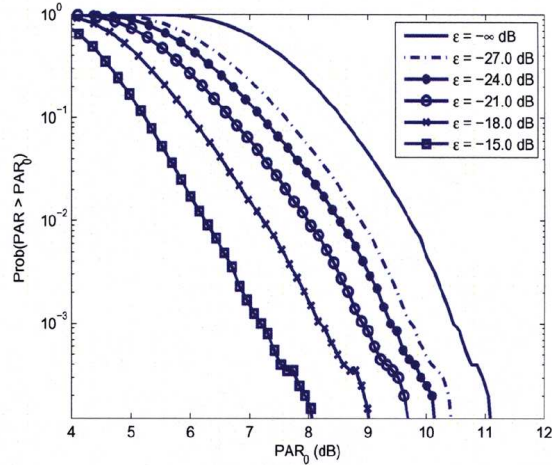
Figure 3.21: PAR CCDF of 16-QAM OFDM using the CD technique as a function of ϵ_{max} [6].

case of DMT in wireline systems, there are, typically, subchannels with SNRs that are too low to send any information, so these subchannels must go unused and are available for PAR reduction. In wireless and underwater systems, however, there is typically no fast, reliable channel-state feedback to dictate whether some subchannels should go unused. Instead, a set of subchannels can be reserved, regardless of the received SNRs, resulting in a bandwidth sacrifice, which may or may not be appropriate, depending on the achievable PAR levels.

Assuming a linear channel, and since symbol demodulation at the receiver is done in the frequency domain in a tone-by-tone basis, the tone-reserved subchannels at the receiver can be discarded at the receiver, whereas the data-bearing subchannels can be used to determine the transmitted bit stream. However, any nonlinearities introduced by either the transmitter, channel, or receiver before symbol demodulation can affect the subchannel orthogonality, and the peak-canceling signal could then affect data decisions.

Problem formulation

The PAR of an OFDM signal can be reduced, using the reserved tones to derive a peak-canceling signal $x(t)$, . Adding to the data-bearing signal produces the new composite signal

$$\tilde{x[n]} \quad = x[n] + c[n] = IDFT X_k + C_k \quad = \frac{1}{\sqrt{(K)}} \sum_{k=0}^{K-1} (d_k + c_k) e^{j2\pi kn/K}$$

where PAR is defined as

$$PAR = \frac{\max |x[n] + c[n]|^2}{E\left\{|x[n]|^2\right\}} \tag{3.32}$$

In the equation above, the denominator is defined as the energy of the original signal. Although it is typically referred to as the PAR problem, the real issue is the peak power at the power amplifiers. Reducing the PAR by inflating the average power does not help. The average power is simply a way of normalizing peak-power results, and this normalization factor should remain constant for comparison purposes.

The vectors X and C are disjoint

$$\mathbf{X} + \mathbf{C} = \left\{ \begin{array}{ll} d_k & \in A \\ c_k & \in A^C \end{array} \right. \tag{3.33}$$
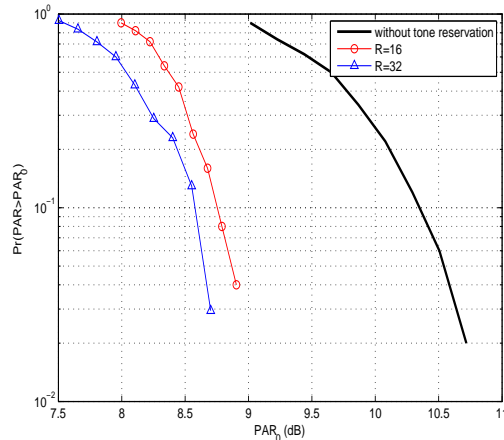
Figure 3.22: CCDF PAR results as a function of the amount of reserved tones R.

where A represents the set of data-bearing subchannels, and A^c represents the set of available subchannels for PAR reduction. It may be desirable to minimize the PAR as much as possible, and given the set A, a minimax PAR optimization problem can be formulated as

$$\min_{c[n/L]} \frac{\max |x[n/L] + c[n/L]|^2}{E\lfloor|x[n/L]|^2\rfloor} \tag{3.34}$$

As it is described in this chapter, PAR must be computed using a discrete oversampled signal in order to predict the peaks in continuous time. Taking into account this fact, the anterior minimization can be rewritten using vectorial notation as

$$\min_{\mathbf{C}} \ \max \ \mathbf{x}_L^m + \boldsymbol{\Phi}\mathbf{c} \tag{3.35}$$

where $\mathbf{x}_L^m$ is the m-th OFDM symbol, $\boldsymbol{\Phi}$ is the oversampled IDFT matrix and $\mathbf{C}$ is the frequency domain signal that we will assign to our set of subcarriers. The optimization problem consists on computing the vector of variables $\mathbf{C} = [C_0, ..., C_{Kp-1}]^T$.

Fortunately, the problem of computing the values for these reserved tones that minimize the PAR can be formulated as a convex problem [8]. The optimal case is obtained by solving a QCPQ for the complex multicarrier case, or by solving an LP case for the real multicarrier case (baseband transmission).

Several solutions have been proposed to solve the system [29]. For example, a low complexity gradient based approach for enabling the Tone Reservation (TR) technique to reduce the PAR in [30].

Results and performance

In the following simulations I set up an OFDM system with $K = 256$ subcarriers, with QPSK modulation in the data-bearing subcarriers and different number of reserved tones. Figure 3.22 shows the PAR of the original signal, along with TR scheme presented here for different number of reserved tones. In the case of original OFDM signal, the reserved tones carry zeros.From Figure 5 we can see that with probability of 10^{-1}, PAR of the original signal is more than 10.4 dB, while for a system with 16 and 32 reserved tones the PAR is reduced approximately to 8.5 dB and 8.6 dB, respectively. With an oversampling rate of 4, the results represent PAR of the analog signal with a good accuracy.

Conclusion

The Tone Reservation technique offers a distortionless technique that efficiently reduces the PAR. Although we have to sacrifice bandwidth, side information is not necessary during the process because the new information is allocated in the orthogonal subcarriers. Hence, at the receiver, the non-data-bearing subcarriers are ignored.
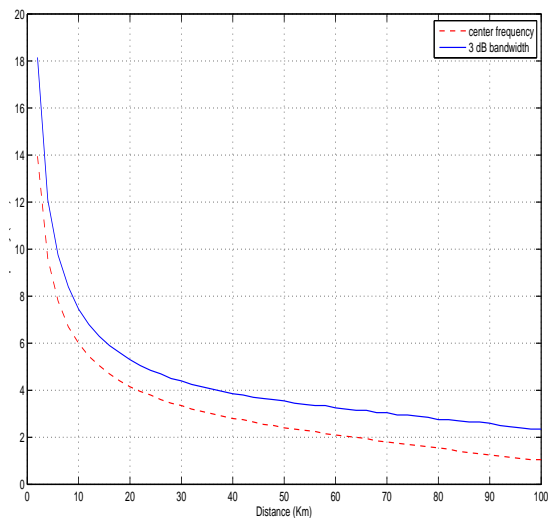
Figure 3.23: Optimal center frequency and the 3 dB acoustic bandwidth as functions of distance [1].

3.4 Differences between acoustic and radio wireless systems

The PAR problematic is always treated for radio wireless environments (e.g. [3, 5, 7, 26]), but it has never explicitly developed for underwater acoustic communications. In this section are highlighted the main differences to take into account when a PAR reduction technique is designed for underwater communications.

The major difference between acoustic and radio systems is in the frequency band that they occupy. Acoustic propagation occurs at frequencies that are much lower than those used for typical radio communications, as illustrated in Fig. 3.23. The bandwidth is fundamentally limited by absorption, but also by the transducer technology, which imposes strict additional limitations.

It is also interesting to note that unlike radio spectrum, acoustic spectrum usage is not legally regulated. This is not to say that one should create interference to neighboring acoustic systems, but simply that acoustic emissions outside of the nominal bandwidth are left to the designer's best effort. When designing a system, it is also important to keep in mind that higher acoustic frequencies attenuate faster with distance, and, hence, the interference spectrum measured at the transmitter will not be the same as that measured at the receiver.

Chapter 4

Proposed technique: Out-of-band tone insertion (OTI) technique

The proposed technique is based on adding a data-block-dependent control signal to the original multicarrier signal. The control signal is outside of the useful bandwidth, and is given by

$$y(t) = \sum_{k=0}^{K_c-1} c_k e^{j2\pi(K+k)\Delta ft}, t \in [0, T] \tag{4.1}$$

where K_c is the number of control tones. The control tones are here placed immediately above the useful bandwidth, but other arrangements are possible as well. The coefficients c_k are chosen so as to reduce the PAR at the input to the non-linear amplifier. The inserted tones are removed after amplification, either by the transducer alone, since it has a limited bandwidth, or by explicit filtering, as illustrated in Fig.4.1. An efficient implementation of the post-amplifier (analog) filter is deemed possible at frequencies used in typical acoustic communication systems.

The main advantage of the OTI technique is that no side information needs to be transmitted, and, hence, there is no trade-off between the data rate loss and the PAR reduction capability.

Although filtering is applied before transmission, there is some amount of power lost in amplifying the inserted signal. Therefore, it is important to maintain the number of out-band inserted tones as low as possible while aiming for a certain PAR reduction.

While the set of reserved tones is chosen in advance, the coefficients c_k are selected depending on the data vector to be transmitted. These coefficients can be chosen optimally (to minimize the PAR) but the computational demands of optimization are high. We will thus investigate other approaches that are sub-optimal, but offer manageable complexity.

Specifically, we want to answer the following questions:

1. Where should the tones be, so that they provide the best performance for all the signals?
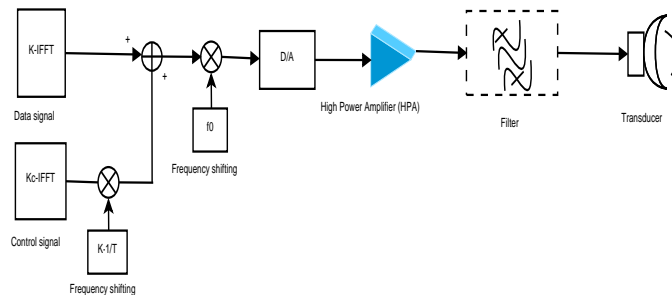

Figure 4.1: Block diagram of the transmitter using out-of-band tone insertion.

2. How many tones are needed in order to achieve a certain improvement?

3. Given a properly chosen number and placement of the inserted tones, how can we efficiently compute the coefficients c_k?

4.0.1 OTI optimal formulation

Mathematically, we can formulate the problem as

$$\min_{\mathbf{c}} \max_{l=0,\ldots N_s-1} |x_l(\mathbf{d}) + y_l(\mathbf{c})| \tag{4.2}$$

where x_l and y_l are the samples of the information-bearing signal (3.2) and the control signal (4.1), which depend on the vector of data symbols $\mathbf{d}$ and the vector of control coefficients $\mathbf{c}$, respectively. The samples of the control signal can also be grouped into a vector,

$$\mathbf{y} = \mathbf{\Phi c} \tag{4.3}$$

where $\mathbf{\Phi}$ is the matrix of $N_s \times K_c$ FFT coefficients

$$\phi_{l,k} = e^{j2\pi l(K+k)/N_s}, l = 0,\ldots N_s - 1,\ k = 0,\ldots K_c - 1 \tag{4.4}$$

Denoting by $\mathbf{\Phi}_l$ the l-th row of $\mathbf{\Phi}$, the optimization problem can be expressed as

$$\min_{\mathbf{c}} \max_{l=0,\ldots N_s-1} |x_l + \mathbf{\Phi}_l \mathbf{c}| \tag{4.5}$$

Fortunately, this proves to be a convex problem, which can be solved numerically using quadratically constrained quadratic programming (QCQP) [8]. Namely, since minimizing an absolute value $|a|$ is the same as minimizing its square $p = |a|^2 = aa^*$, the problem can be re-formulated as

$$\min_{\mathbf{c}} p, \text{ subject to } [x_l + \mathbf{\Phi}_l \mathbf{c}][x_l + \mathbf{\Phi}_l \mathbf{c}]^* \le p,$$
$$\text{for } l = 0,\ldots N_s - 1 \tag{4.6}$$

This formulation involves minimization of a linear function over a set of quadratic constraints, which is a convex problem [8]. In what follows, we will refer to this solution as the optimal solution, and use it as a benchmark to compare the performance of other techniques whose computational demands are conducive to practical implementation. Two such techniques are discussed below.

4.0.2 Gradient technique

This technique substitutes the (optimal) criterion of PAR minimization by the (suboptimal) minimum mean squared error (MMSE) criterion applied to the clipping noise. A gradient algorithm is then applied to solve the MMSE optimization in a fast and computationally efficient manner.

To arrive at this algorithm, let us first define the passband signals

$$\begin{aligned} \tilde{x}(t) &= Re\{x(t)e^{j2\pi f_0 t}\} \\ \tilde{y}(t) &= Re\{y(t)e^{j2\pi f_0 t}\} \end{aligned} \tag{4.7}$$

as well as the composite signal $\tilde{z}(t) = \tilde{x}(t) + \tilde{y}(t)$, which is input to the power amplifier. The amplifier non-linearity is modeled as

$$\bar{\tilde{z}}(t) = g[\tilde{z}(t)] = \begin{cases} \tilde{z}(t), & |\tilde{z}(t)| \le A \\ A, & \tilde{z}(t) > A \\ -A, & \tilde{z}(t) < -A \end{cases} \tag{4.8}$$

The resulting error, i.e. the clipping noise, is given by

$$\tilde{e}(t) = \tilde{z}(t) - \bar{\tilde{z}}(t) \tag{4.9}$$

and the corresponding MSE is defined as

$$D = \int_0^T |\tilde{e}(t)|^2 dt \tag{4.10}$$

Taking the derivative of D with respect to the control coefficients c_k, we obtain

$$\frac{\partial D}{\partial c_k} = 2 \int_0^T \tilde{e}(t) \frac{\partial \tilde{e}(t)}{\partial c_k} dt \tag{4.11}$$

The integration interval can be split into two complementary parts: $\mathcal{T}$, in which $|\tilde{z}(t)| \leq A$, and $\overline{\mathcal{T}}$, in which clipping occurs. Since the error is zero in the first part, only the second part will contribute to the MSE. In that part, the error is given by $\tilde{e}(t) = \tilde{z}(t) \pm A$, and, hence,

$$\frac{\partial \tilde{e}(t)}{\partial c_k} = \frac{\partial \tilde{e}(t)}{\partial \tilde{z}(t)} \frac{\partial \tilde{z}(t)}{\partial c_k} = \frac{\partial \tilde{z}(t)}{\partial c_k} \tag{4.12}$$

The remaining term is obtained as

$$\frac{\partial \tilde{z}(t)}{\partial c_k} = \frac{1}{2} \phi_k^*(t) e^{-j2\pi f_0 t} \tag{4.13}$$

where

$$\phi_k(t) = e^{j2\pi(K + k\Delta f)t} \tag{4.14}$$

We thus finally have the MSE gradient,

$$\frac{\partial D}{\partial c_k} = \int_0^T \tilde{e}(t) \phi_k^*(t) e^{-j2\pi f_0 t} dt \tag{4.15}$$

In this expression, we have switched the integration bounds from $\overline{\mathcal{T}}$ back to the original ones, as this does not affect the result since $\tilde{e}(t) = 0$ outside of $\overline{\mathcal{T}}$.

Further simplification of the above expression is also possible if we express the passband error as

$$\tilde{e}(t) = Re\{e(t) e^{j2\pi f_0 t}\} \tag{4.16}$$

where $e(t)$ is the complex equivalent evaluated with respect to f_0. Substituting this expression into the gradient (4.15), the high-frequency terms at $2f_0$ vanish under integration, leaving

$$\frac{\partial D}{\partial c_k} = \frac{1}{2} \int_0^T e(t) \phi_k^*(t) dt \tag{4.17}$$

The complex envelope $e(t)$ can be related to an equivalent baseband non-linearity, described by the AM/AM and AM/PM characteristic g_0 corresponding to the nonlinearity g, such that $e(t) = z(t) - g_0[z(t)]$. For the hard limiter model (4.8), this function is given by [20]

$$\bar{z}(t) = g_0[z(t)] = \begin{cases} z(t), & |z(t)| \leq A \\ \frac{4}{\pi} A e^{j \arg[z(t)]}, & |z(t)| > A \end{cases} \tag{4.18}$$

Once the gradient (4.17) is known, the least mean squares (LMS) algorithm can be applied to calculate the coefficients c_k. The gradient will be calculated in discrete time, giving way to the coefficient update

$$c_k(i+1) = c_k(i) - \mu \sum_{l=0}^{N_s-1} e_l(i) \phi_{l,k}^* \tag{4.19}$$

where μ is the step size, $e_l(i)$ is the clipping error in the i-th iteration, and $\phi_{l,k}$ are as given in the expression (4.4). Using the notation of Sec.4.0.1, the vector update is given by

$$\mathbf{c}(i+1) = \mathbf{c}(i) - \mu \sum_{l=0}^{N_s-1} e_l(i) \mathbf{\Phi}_l' \tag{4.20}$$

Instead of generating the control signal from the coefficients after the algorithm has converged, the signal itself can be updated [8]. The LMS algorithm will then operate in the time domain, directly generating the signal vector $\mathbf{z} = \mathbf{x} + \mathbf{y}$. The corresponding update equation is obtained by multiplying both sides of the expression (4.20) by the FFT matrix $\mathbf{\Phi}$, and adding the information bearing signal:

$$\mathbf{z}(i+1) = \mathbf{z}(i) - \mu \sum_{l=0}^{N_s-1} e_l(i)\mathbf{\Phi}\mathbf{\Phi}'_l \tag{4.21}$$

Since the error depends only on the signal, $e_l(i) = z_l(i) - \bar{z}_l(i)$, the control coefficients never need to be computed explicitly. The algorithm is initialized by $\mathbf{z}(0) = \mathbf{x}$. The vectors $\mathbf{\Phi}\mathbf{\Phi}'_l$, $l = 0, \ldots N_s - 1$, can be pre-computed and stored, which accounts for the very low computational complexity of the algorithm. The LMS convergence time, nominally $20N_s$ iterations, amounts to $80K$ iterations with the oversampling ratio of 4. These iterations need to be completed within the duration of one block, $T = K/B$, in order for a real time implementation to be possible. If we take as an example a 160 MHz processor, this will be possible so long as 160 MHz/$80B$=$2/B$[MHz] is greater than the number of instructions required per iteration. As we shall see from the simulation results, it suffices to perform only a few iterations.

The algorithm

In this subsection, the main points of the algorithm are summarized as follows:

- **Initialization**: These steps only need to be executed once.

    1. Select the target PAR value or ,equivalently, the desired level A.

    2. Choose the set of inserted tones K_c. The receiver does not need to know that these tones are not used for data transmission.

    3. Compute and store the kernel vector $\mathbf{\Phi}\mathbf{\Phi}'_l$

- **Run time**: This algorithm is invoked for each multicarrier symbol that exceeds the desired PAR. For each OFDM block:

    1. Initial condition: set $\mathbf{z}(0) = \mathbf{x}$.

    2. Compute the error on the signal $e_l(i) = z_l(i) - \bar{z}_l(i)$. If the previous error is equal to zero, Jump to 5

    3. Update $\mathbf{z}(i)$ according to

$$\mathbf{z}(i+1) = \mathbf{z}(i) - \mu \sum_{l=0}^{N_s-1} e_l(i)\mathbf{\Phi}\mathbf{\Phi}'_l \tag{4.22}$$

    4. Increment the iteration counter i=i+1. If i<MaxIterations, Jump to 2.

    5. Transmit $\mathbf{z}(i)$

4.0.3 Random insertion

In this technique, the out-of-band tones are generated from a finite modulation alphabet, which can be the same as that of the information-bearing signal, or different. Thus, there is a finite number of possible selections for the control sequence, but this number may be large (M^{K_c} for the modulation level M), making it impractical to conduct an exhaustive search.

Instead of performing a systematic search, the selection is made from a finite set of randomly generated control sequences. The search for the best sequence is conducted until a certain improvement in the PAR is reached, or until a pre-determined number of trials have been exhausted (after which the best candidate sequence is retained).

Random tone insertion aims to reduce the implementation complexity by sacrificing some improvement in the PAR reduction capability. This technique is similar to interleaving [9] in that the transmitter only
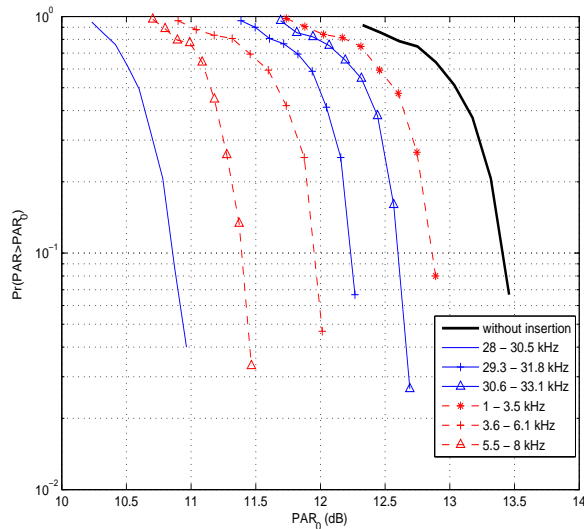
Figure 4.2: CCDF of the PAR when control tones are inserted above the useful bandwidth (solid) and below the useful bandwidth (dashed). Legend indicates the bandwidth occupied by the control signal.

needs a random generator for the out-of-band tones and a module that computes the PAR. Note, however, that the two techniques are conceptually different, and can even be combined.

Two specific questions are to be addressed with this technique. The first question refers to the size of the control sequence alphabet. The greater the alphabet size, the better the PAR reduction (the optimal solution described in Sec.4.0.1 can in fact be regarded as a modulation with an infinite constellation size). However, an increase in the modulation alphabet implies a greater number of candidate sequences, which complicates the search. The second question refers to the number of trials needed to achieve a certain performance. Obviously, the more trials, the better, but we would like to know how much can the performance be improved with a relatively small number of trials, suitable for a practical implementation. These questions will be addresses in the following section.

4.1 Simulations results

A simulation analysis was conducted for an OFDM signal with 512 carriers employing QPSK in the 8-28 kHz band. A total of 10,000 randomly generated OFDM blocks were used to assess the performance of the proposed OTI techniques. The results are contrasted with the original signals' statistics (no PAR reduction method employed) and the optimal case, which was evaluated according to the principles of Sec.4.0.1.

4.1.1 Control bandwidth allocation

The out-of-band tones can be placed either below or above the useful bandwidth, and the question is which is better. Fig. 4.2 shows the system performance under different allocation policies. Indicated in the figure is the bandwidth occupied by the control signal consisting of 64 tones. Clearly, allocating the control signal above the useful bandwidth results in a better performance. Moreover, the control tones are best placed as close as possible to the upper edge of the data bandwidth. Ideally, no separation between the two bands should be used, although some separation may be required to keep the radiated out-of-band acoustic power below a pre-specified level.
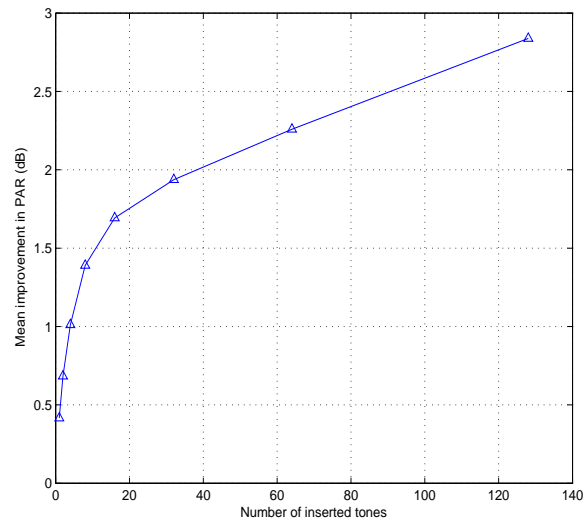
Figure 4.3: PAR improvement vs. the number of out-of-band tones.

4.1.2 Number of control tones

Given the control signal placement at the upper edge of the useful bandwidth, we now want to determine the minimum number of control tones needed to ensure a certain PAR reduction. Note that there is a trade-off here, as more tones enable better control of the peak power, but increase the overall average power. The relationship between the number of control tones and the achievable improvement is depicted in Fig. 4.3. The average achievable improvement is defined as the average PAR reduction achieved using the optimal control signal. This result quantifies the effect of diminishing returns that takes place as the number of control tones is increased, but it also demonstrates that an improvement of several dB is available from the OTI technique with a reasonably small number of control tones.

Below, we address the performance of practical OTI techniques, namely the gradient technique and the random insertion technique.

4.1.3 OTI–Gradient technique

The gradient algorithm described in Sec.4.0.2 was applied to each incoming data block until its original PAR was reduced by 4 dB, or a pre-determined number of trials has been reached, whichever came first. For each incoming OFDM block, the step size was chosen as $\mu = 2/K$.

Fig. 4.4 shows the performance of the gradient technique, obtained after a varying number of LMS iterations. The PAR reduction achieved after the first few iterations is outstanding, with diminishing improvement thereafter. For example, a 2.5 dB reduction is obtained after only three iterations when the original PAR is 13 dB.

Performance of the gradient technique is further illustrated in Fig.4.5, which shows the normalized MSE, i.e. the variance of the clipping error obtained after a given number of iterations, averaged over all data blocks. These results demonstrate that a considerable improvement is available from the OTI technique at a very low computational cost.

4.1.4 OTI–Random insertion

Fig. 4.6 shows the results obtained using the random insertion technique described in Sec.4.0.3. The maximal number of trials (randomly generated control sequences) is set to 100, and the modulation method (alphabet size) used for the control signal is varied. The data sequence is modulated using QPSK. Interestingly, there is not much to be gained by increasing the modulation level from 2 to 16. This fact justifies the use of simple
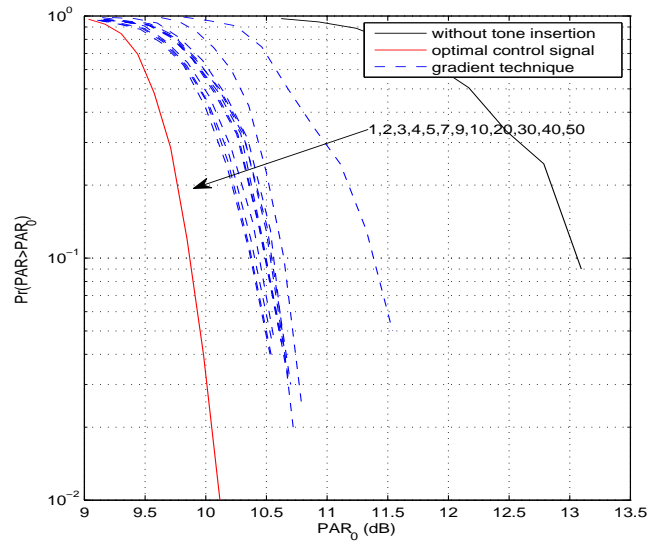
Figure 4.4: CCDF of the PAR resulting from the gradient technique after a varying number of iterations.
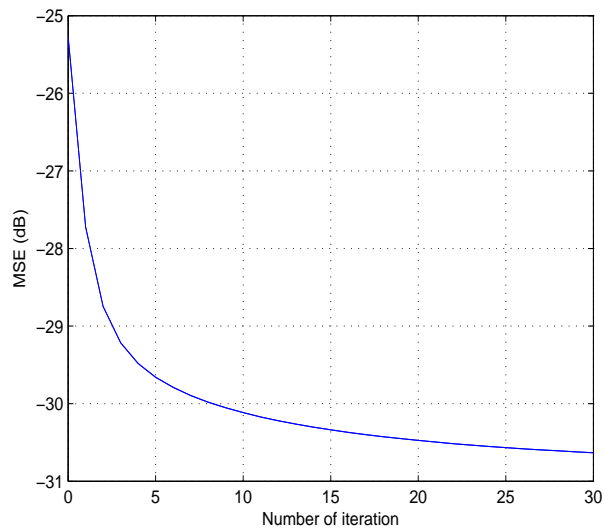

Figure 4.5: Normalized MSE of the gradient technique.
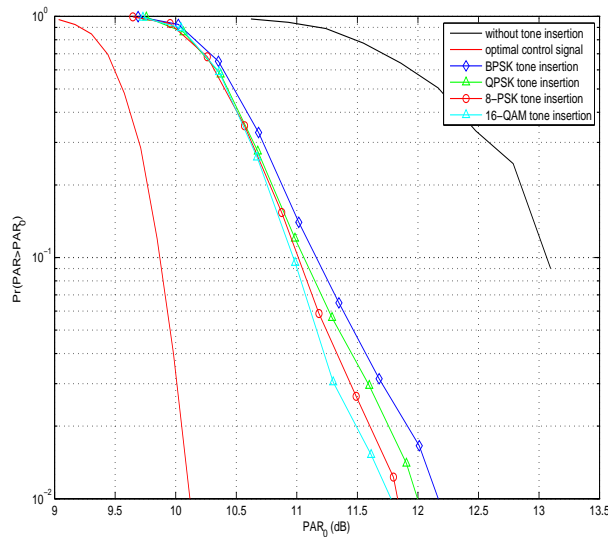
Figure 4.6: CCDF of the PAR resulting from random insertion technique. The data sequence is modulated using QPSK, and the number of trials is limited to 100.

control sequences, such as BPSK or QPSK. We also note that the overall PAR reduction is comparable to that obtained using the gradient technique.

The question of the number of trials needed to achieve a certain performance is addressed in Fig.4.7. Similarly as with the number of iterations in the gradient technique, we observe an effect of diminishing returns with the number of trials here. However, the results are somewhat less encouraging, since at least a few tens of trials are needed to achieve a substantial improvement. At a (hypothetical) 1000 trials, the performance deviates from the optimal by about 0.75 dB. In comparison, the gradient technique achieves this in about ten iterations.

4.2 OTI − Conclusions

Out-of-band Tone Insertion was presented as a practical means for reducing the large PAR in the OFDM signals. Two approaches have been proposed to implement the idea: a gradient technique (GFC) by formulating the PAR problem as a convex problem and a sub-optimal alternative (RI) based on generating a predetermined number of random sequences.

I studied the impact of the number of candidate sequences, their constellation, as well as the location of the out-of-band tones. Numerical analysis shows that the best tone allocation appears to be at the high frequency end, close to the data bandwidth. The results of the technique illustrate the tradeoff between PAR reduction and the amount of inserted tones, which results in energy consumption.

The proposed OTI-GFC method offers a faster reduction compared to the Optimal Resolution Case. The cost associated with a GFC iteration is $O((K + K_p))$, which is smaller than the basic $O((K + K_p)^3)$ cost by inverting the matrix of the equation. Since only two or three iterations of the OTI-GFC approach are needed (further iterations produce negligible results), it makes the algorithm practical for future implementations.

In contrast with GFC, the cost to evaluate each inserted tone in RI is $O((K + K_p)log(K + K_p))$. However, the random insertion offers an easier implementation to reduce the PAR. The results are comparable to the GFC technique, but with small reduction in PAR improvement.
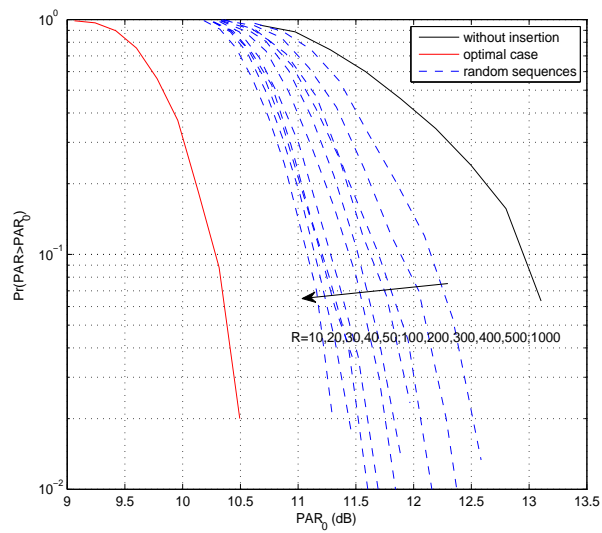
Figure 4.7: CCDF of the PAR resulting from random insertion technique with a varying number of trials. The data and the control sequence are modulated using QPSK.

4.3 Comparison with other techniques

There are many factors that should be considered before a specific PAR reduction technique is chosen. This section discusses the main elements which have to be taken into account when selecting a PAR reduction technique for a specific system. The key parameters of a PAR reduction technique follow along with the comparison of the OTI technique to other techniques.

- ***PAR reduction capability***: Clearly, this is the most important factor in choosing a PAR reduction technique. Careful attention must be paid to the fact that some techniques result in other harmful effects. For example, the amplitude clipping technique clearly removes the time domain signal peaks, but results in in-band distortion and out-of-band radiation.

- ***Power increase in the transmitted signal***: Some techniques require a power increase in the transmitted signal after using PAR reduction techniques. For example, TR requires more signal power because some of its power is reserved for optimization. ACE constellation points require more power than the original constellation point, the transmitted signal will have more power after applying ACE. When the transmitted signal power is equal to or less than the one before using a PAR reduction technique, the transmitted signal should be normalized back to the original power level, resulting in BER performance degradation for these techniques.

- ***BER increase at the receiver***: This is also an important factor and closely related to the power increase in the transmitted signal as explained above. In some other techniques such as SLM, PTS, and interleaving, the entire data block may be lost if the side information is received in error. This may also increase the BER at the receiver.

- ***Loss in data rate***: Some techniques require the data rate to be reduced. In SLM, PTS, and interleaving, the data rate is reduced due to the side information used to inform the receiver of what has been done in the transmitter. Furthermore, in these techniques must employ coding in order to protect the side information, thus resulting in an extra loss in data rate.

- ***Computational complexity***: Computational complexity is another important consideration in selecting a PAR reduction technique. Techniques such as PTS find a solution for the PAR reduced signal by using many iterations. The PAR reduction capability of the interleaving technique is better for a larger number of interleavers. Generally, more complex techniques have better PAR reduction capability.

- ***Other considerations***: Many PAR reduction techniques do not consider the effect of many components in the transmitter such as the transmit filter, digital-to-analog converter (DAC), and transmit power amplifier. In practice, PAR reduction techniques can be used only after careful performance and cost analysis for realistic environments. For example, in the paper

  , the consequences of the transmission filter in PAR reduction are studied in order to obtain maximal PAR reduction.

In Table 4.1, the different parameters are compared among the different techniques which have been proposed. Based on the main parameters these techniques can be mainly categorized into signal scrambling techniques and signal distortion techniques. Signal scrambling techniques are all variations on how to scramble the codes to decrease the PAR. The signal scrambling techniques can be classified into:

- Schemes with explicit side information. Examples: SLM, PTS, Interleaving schemes.

- Schemes without side information. Examples: Block coding scheme and Tone Reservation (TR).

Signal scrambling techniques with side information reduce the effective throughput because they introduce redundancy.

On the other hand, the signal distortion techniques introduce either in-band or out-of-band interference and complexity to the system. The signal distortion techniques reduce high peaks directly by distorting the signal prior to amplification. Examples: ACE and clipping and filtering.

This work proposes a novel scrambling algorithm based in the use of out-of-band inserted tones to significantly reduce the PAR. In Table 4.1, the main characteristics of the OTI technique are summarized. The OTI technique is a distortionless technique because it does not modify the original signal. Furthermore, it does not require side information neither a loss in data rate because the tones are allocated out of band. Furthermore, the increase in complexity is minimum in the transmitter. In the case of the receiver, it remains equal because the the inserted tones are discarded at the beginning.

	Distortion	Data rate loss	Side information	Power increase	Requires processing at Tx or Rx
Clipping and filtering	Yes	No	No	No	Tx: Amplitude clipping, filtering Rx: None
Active Constellation	Yes	No	No	Yes	Tx: IFFTs, projection onto shaded "area" Rx: None
Selected Mapping	No	Yes	Yes	No	Tx: U IFFTs Rx: Side information extraction, inverse SLM algorithm
Interleaving	No	Yes	Yes	No	Tx: K IFFTS, (K-1) interleavers Rx: Side information extraction , inverse Interleaving
Tone Reservation	No	Yes	No	Yes	Tx: IFFTS, find the value of the pilots Rx: Ignore non-data-bearing subcarriers
Out-of-band tone insertion	No	No	No	Yes	Tx: IFFTS, find the value of the pilots Rx: Ignore out-of-band subcarriers

Table 4.1: Comparison of PAR reduction techniques

Chapter 5

Conclusions and Further work

When using OFDM in transmission systems, the transmitted signal will occasionally exhibit very high peaks. Nonlinearities may become overloaded, causing intermodulation among the subcarriers and - more critical - undesired out-of-band radiation. If power amplifiers are not operated with large power back-offs, it is impossible to keep the out-of-band power below imposed limits which creates very inefficiencies. Very inefficient amplification and expensive transmitters result. Thus, it is highly desirable to reduce the peak power.

The first part of this work describes some PAR reduction techniques for multicarrier transmission. Many promising techniques to reduce PAR have been proposed, all of which have the potential to provide substantial reduction in PAR at the cost of loss in data rate, transmitted signal power increase, BER increase, computational complexity increase, and so on.

No specific PAR reduction technique is the best solution for all multicarrier transmission systems. However, the PAR reduction technique should be carefully chosen according to various system requirements. In practice, the effect of the transmission filter, D/A converter, and the power amplifier must be taken into consideration in order to choose an appropriate PAR reduction technique.

In the second part, out-of-band tone insertion was proposed as a PAR reduction technique for underwater acoustic OFDM systems. A set of tones is inserted outside of the nominal signal bandwidth prior to D/A conversion. The control tones are digitally optimized to provide PAR reduction before the signal is D/A converted and fed to the (nonlinear) power amplifier. The tones are subsequently removed by the transducer which acts as a filer, or by explicit filtering. The main advantage of the technique proposed is that PAR improvement comes at no reduction in the data rate.

Two approaches were considered for computationally-efficient design of the control signal: a gradient technique which minimizes the mean-squared clipping error, and a random insertion technique in which the selection of control signal is made from a finite set of randomly generated symbols. The performance of these techniques, as well as the number and placement of control tones, were studied via a numerical analysis.

Results show that the best tone placement is at the high end of the useful signal bandwidth. The improvement in PAR reduction grows with the number of tones, but there is an effect of (exponentially) diminishing returns, which justifies the use of a relatively small number of tones (not more than what is used for the information signal). Both the gradient technique and random insertion offer non-negligible PAR improvements. The gradient technique exhibits fast convergence, yielding a close-to-optimal solution in only a few LMS iterations. Random insertion offers a comparable, albeit slightly inferior performance, using control symbols from the same alphabet as the data symbols (QPSK), and a search limited to about a hundred sequences.

There is the possibility that a single PAR reduction technique may not reach the desired results. Future work on PAR reduction techniques for underwater communications should focus on studying the impact of combining different techniques. Since the OTI technique does not require side information, it can be perfectly

combined with other techniques which require side information such as Interleaving, PTS or SLM.

Future work should also focus on implementing the OTI in a real system. Testing the OTI technique in an AUV is the best way to contrast results. There are a few questions which remain opened: the amount of power consumed by the inserted tones in the power amplifier and the effectiveness of the filtration to cancel the out-of-band signal.

There is the possibility future work is the study of combining the OTI technique with the idea introduced by Jovana Ilic and Thomas Strohmer in [31]. In this paper, it is presented an idea which combines the properties of sparse signals with properties of the Uncertainty Principle that are related to multiple sub-carrier signals. They design an efficient iterative method for constructing OFDM signals with lower PAR. Unlike most existing subcarrier reservation methods, their method provides a guaranteed upper bound for PAR reduction as well as guaranteed rates of convergence. Combining both techniques could be possible to guarantee an upper bound for PAR reduction without a loss in data rate.

Appendix A

Scripts

In this section, the scripts to compute the Out-of-band technique can be found.

A.1   OTI- Gradient technique's script

```
%%%%%%%%%%%%%% Script: gradient_technique.m %%%%%%%%%%%%%%%%%%
%Out-of-Band Tone insertion best value, Gradient technique%%

%% COMMON VARIABLES%%
M=4; % modulation level (4,8,16 QAM) in K subcarriers
K=512; % number of channels (128,256,512,1024,2048)
Kp=64; % number of inserted tones
Ns=4*K;
Nd=K; % total number of data symbols to be tx (mult. of K)
ldM=log2(M);
Nb=Nd*log2(M); % number of bits in packet

%%%% MODULATION %%%%%%%
f1=10000; % first carrier (2f0>B:ok)
fs=96000; % sampling freq. (Jim's)
Up= exp(j*2*pi*f1/fs*(0:8*K-1));

%% VARIABLES IN THE SIMULATION%%

FINAL=500; % Number of simulations
ITERATIONS_MAX=30;%%% Maximum iterations
DIFF=3; %%%Threshold value, 4 dB is shown to be a good value
experiment='Experiment-5' %%name to save
dibuixar_altres=1; %%% plotting other graphics
threshold_f=40.1902; %% Reference level in MSE
mhu=2/K


%% INICIALIZATION PROCESS%%
% First time has to be executed the inizialization code, then we can save
% in a variable and use it later.

%%%%%%%%%%%%%%%%%%FIRST TIME%%%%%%%%%%%%%%%%%%%%%%
 E = exp(j*2*pi/(8*K)*(0:(8*K-1))'*[1:K]);
```

```
 Q = exp(j*2*pi/(8*K)*(0:(8*K-1))'*[K+1:K+Kp]);

% %
   for m=1:8*K
       p(m,:)=Q*Q(m,:)';
   end

 save p_last p

% %%%%%%%%%%%%%%OTHER TIMES%%%%%%%%%%%%%%%%%%%
% load p_last;
% whos p_last;
%%%%%%%%%%%%%%%%%%%%%%%%%%%%%%%%%%%%%%%%%%%%

%% RUN TIME %%
for z=1:FINAL


    Progress=z/FINAL*100

    b=pn(16,Nb,z); % binary (0,1) information sequence
    Bb=reshape(b,ldM,Nd); % ldM bit streams;
    % map bits into symbols
    if M==2; d=2*b-1; end;
    if M==4; d=grmap4psk(Bb); end;

    u(1,:)=E*d.';
    u(1,:)=real(u(1,:).*Up);
    P0(z,1)=10*log10(compute_PARP(u(1,:),u(1,:)));


for i=1:ITERATIONS_MAX


   if(i==1);  threshold=max(abs(u(1,:)))*10^(-DIFF/20);  end;
    res=abs(u(i,:))>(threshold);

     %if(sum(res)==0); finaliterar(z)=i, break; end;

    w=(u(i,:)- (threshold)*exp(j*phase(u(i,:)))).*res;

    acumulat(1,:)=zeros(size(u(i,:)));
    acumulatfinal(1,:)=zeros(size(u(i,:)));

    if(dibuixar_altres==1)

        res2=abs(u(i,:))>threshold_f;
        w2=(u(i,:)- (threshold_f)*exp(j*phase(u(i,:)))).*res2;
        MSE(z,i)= 10*log10(pwr(w2)/pwr(u(1,:)));
    end

for m=1:length(u(1,:))
    if(w(m)~=0)
    vector(m,:)=w(m).*p(m,:);
```

```
    acumulat=acumulat-mhu*vector(m,:);
    end;
end
    if(dibuixar_altres==1); acumulatfinal=acumulatfinal+acumulat; end;

    u(i+1,:)=u(i,:)+acumulat;
    u(i+1,:)=real(u(i+1,:));

    P0(z,i+1)=10*log10(compute_PARP(u(i+1,:),u(1,:)));

end

    %%%LAST ITERATION MSE%%%%%%%
    if(dibuixar_altres==1)
        res2=abs(u(ITERATIONS_MAX,:))>threshold_f;
        w2=(u(ITERATIONS_MAX+1,:)- (threshold_f)*exp(j*phase(u(ITERATIONS_MAX+1,:)))).*res2;
        MSE(z,ITERATIONS_MAX+1)= 10*log10(pwr(w2)/pwr(u(1,:)));
    end
        %%%%%%%%%%%%%%%%%%%%%%%%%%%%%%%%%

end

%% Plot Process%%


%%%%VARIABLES FOR PLOTTING%%%%%%
color=['b--';'bx-';'bx-';'b--';'b--'];%% Figure properties
mostrar=[1,2,3,4,5,7,9,10,30];

%%%%%%%%%%%%%%%%%%%%%%%%%%%%%%%%%%%%

[N0, X0]=hist(P0(:,1));
figure(1), semilogy(X0,1-cumsum(N0)./sum(N0), 'k')

%%% Plotting the optimal value%%%
%load optimal_oversampling
%[N1, X1]=hist(10*log10(new));
%figure(1),hold on, semilogy(X1,1-cumsum(N1)./sum(N1), 'r');



for m=1:length(mostrar)
    [N(m,:), X(m,:)]=hist(P0(:, (mostrar(m)+1) ));
    figure(1), hold on;
    semilogy(X(m,:),1-cumsum(N(m,:))./sum(N(m,:)), color(1,:))
end

xlabel('PAR_0 (dB)')
ylabel('Pr(PAR>PAR_0)')
legend('original signal, no PAR reduction', 'optimal solution ','gradient technique')
% titul=sprintf('%s Parameters are Mu= %d and Improvement target is %d (dB)',experiment, mhu, DIFF);
% title(titul);
```

```
%%%%%%%Evolucio%%%%%%%%%%%%%%%%%%%
figure(2),hold on;
mitjes=mean(P0(:,:))
plot(mitjes(1:length(mitjes)),color(2,1));
xlabel('Iteration')
ylabel('PAR on average (dB)')
% titul=sprintf('%s Parameters are Mu= %d and Improvement target is %d (dB)',experiment, mhu, DIFF);
% title(titul);

figure(3),hold on;
diff=mitjes(1:length(mitjes)-1)-mitjes(2:length(mitjes));
plot(diff,color(3,1))
xlabel('Number of iteration')
ylabel('Improvement/Iteration')
% titul=sprintf('%s Parameters are Mu= %d and Improvement target is %d (dB)',experiment, mhu, DIFF);
% title(titul);


if(dibuixar_altres==1)
%%%%%%%%%Plotting signals...%%%%%%%%%%%%%%%%%%
figure(5),hold on;
subplot(3,1,3),plot(real(u(i+1,:))), ylabel('Amplitude'), xlabel('Samples'), legend('Signal x[n]+c[n]')
subplot(3,1,1), plot(real(u(1,:))), ylabel('Amplitude'), xlabel('Samples'), legend('Signal x[n]')
subplot(3,1,2),plot(real(acumulatfinal),color(5,1)), ylabel('Amplitude'), xlabel('Samples'), legend('Sig
%subplot(4,1,2),plot(real(acumulatfinal(2,:)),color(5,1))

%  figure(6)
% subplot(4,1,4),plot(10*log10(abs(fft(xcorr(real(u(i+1,:)),length(u(i+1,:)))))))
% subplot(4,1,1), plot(10*log10(abs(fft(xcorr(real(u(1,:)),length(u(1,:)))))))
% subplot(4,1,3),plot(10*log10(abs(fft(xcorr(real(acumulatfinal(i+1,:)),length(u(1,:)))))))
% subplot(4,1,2),plot(10*log10(abs(fft(xcorr(real(acumulatfinal(2,:)),length(u(1,:)))))))
 end

figure(7),hold on;
MSE_m=mean(MSE(:,:));
plot([0:length(MSE_m)-1],MSE_m,color(4,1))
xlabel('Number of iteration')
ylabel('MSE (dB)')
grid;
% titul=sprintf('%s Parameters are Mu= %d and Improvement target is %d (dB)',experiment, mhu, DIFF);


%% SAVING VALUES
%save(experiment, 'mostrar','P0','mhu','DIFF','FINAL','new')
```

A.2   OTI-Random Insertion's script

```
%%%%%%%%%%%%%%% Script: Random_Insertion.m %%%%%%%%%%%%%%%%%
%%%% OTI -- Random Insertion %%%%%
M=4; % modulation level (4,8,16 QAM)
K=512; % number of channels (128,256,512,1024,2048)
%B=12000;
%df=B/K; % channel separation
%T=1/df; % symbol duration in each channel
```

```
Kp=64; % number of additional active subbands
%bend=1; % o if those bands are adjacent to useful; 1 if they are away
%fs=4*B;
%Ns=T*fs; % samples per subcarrier symbol = K*fs/B, want 2^n for fft
Ns=4*K;
Nd=K; % total number of data symbols to be tx (mult. of K)
ldM=log2(M);
Nb=Nd*log2(M); % number of bits in packet
experiment=1; %number_of_experiment
N_opt=2;%number of possible bendings (has to be multiple of K-Kp)
threshold_f=40.1902;


%%%% MODULATION %%%%%%
f1=10000; % first carrier (2f0>B:ok)
fs=96000; % sampling freq. (Jim's)
Up= exp(j*2*pi*f1/fs*(0:8*K-1));


SIM=3500;
MAXITERATIONS=100;
total=5;

for modulation=5:total

    Proces=modulation/total*100

    color=['b','r', 'g','m', 'c']
    M2=2^(modulation);
    Nd2=Kp;
    ldM2=log2(M2);
    Nb2=Nd2*log2(M2);


for z=1:SIM

    Proces2=z/SIM*100

b=pn(16,Nb,z); % binary (0,1) information sequence
Bb=reshape(b,ldM,Nd); % ldM bit streams;
d=grmap4psk(Bb);
u0=E*d.';
u0=real(u0.*Up);
P0(z)=compute_PARP(u0,u0);


%%%% Adding the new signal %%%%%%%
    for it=1:MAXITERATIONS

        if M2==2
            b2=pn(16,Nb2,it);
          d2=2*b2-1;

        elseif M2==4
            b2=pn(16,Nb2,it); % binary (0,1) information sequence
            Bb=reshape(b2,ldM2,Nd2); % ldM bit streams; end;
```

```
        Bb2=1*Bb(1,:)+2*Bb(2,:);
        d2=pskmod(Bb2,4);

    elseif M2==8
        b=pn(16,Nb2,it);
        Bb=reshape(b,ldM2,Nd2);
        Bb2=1*Bb(1,:)+2*Bb(2,:)+4*Bb(3,:);
        d2=pskmod(Bb2,8);


    elseif M2==16
        b=pn(16,Nb2,it);
        Bb=reshape(b,ldM2,Nd2);
        Bb2=1*Bb(1,:)+2*Bb(2,:)+4*Bb(3,:)+8*Bb(4,:);
        d2=pskmod(Bb2,M2);
        %%% Energy normalization %%%
    else
        b=pn(16,Nb2,it);
        Bb=reshape(b,ldM2,Nd2);
        Bb2=1*Bb(1,:)+2*Bb(2,:)+4*Bb(3,:)+8*Bb(4,:)+16*Bb(5,:);
        d2=pskmod(Bb2,M2);
        %%% Energy normalization %%%
    end

    u=real((E*d.'+Q*d2.').*Up);

    parp(it)=max(abs(u))^2/256;


    end

    min_PAPR2(modulation,z)=min(parp);




end


%    for m=1:MAXITERATIONS
%
%        MSE_ave(modulation,m) = mean(minim(1:50,m));
%
%    end


%%%%%%%%%%%%%Plot the achievable difference%%%%%%%%%
%figure(1);
%plot(10*log10(min_Diff),color(modulation));
%grid;
```

```
%differential_average(bend+1)=mean(10*log10(min_Diff))
%differential_variance(bend+1)=var(10*log10(min_Diff))


%%%%%% PLOT Complementary Cumalative function and histogram%%%%%%%%%%%%%%

% [N0, X0]=hist(10*log10(P0));
% [N(modulation,:), X(modulation,:)]=hist(10*log10(min_PAPR));
%
% figure(2)
% subplot(total,1,modulation)
% plot(X0,N0, 'k', X(modulation,:), N(modulation,:), color(modulation) );
% title('Histogram of PAPR, ')
% legend('original PAPR', 'reduced PAPR')
%
% PAPR_average(modulation)=mean(10*log10(min_PAPR))
% PAPR_variance(modulation)=var(10*log10(min_PAPR))
%
% figure(3)
% subplot(total,1,modulation)
% semilogy(X0,1-cumsum(N0)./sum(N0), 'k' ,X(modulation,:),1-cumsum(N(modulation,:))./sum(N(modulation,:
%
% figure(4)
% hold on
% semilogy(X0,1-cumsum(N0)./sum(N0), 'k' ,X(modulation,:),1-cumsum(N(modulation,:))./sum(N(modulation,:
end

[N0, X0]= hist(old)

for m=1:3

    [N(m,:), X(m,:)]=hist(10*log10(min_PAPR_part1(m,:)))

end

for m=4:5

    [N(m,:), X(m,:)]=hist(10*log10(min_PAPR_part2(m,:)))

end

figure(5), semilogy(X0,1-cumsum(N0)./sum(N0), 'k' ,X(1,:),1-cumsum(N(1,:))./sum(N(1,:)), 'd-b', X(2,:),1
%%%%%%%%%%%%%%%%%%%%%%%%%%%%%%%%%%%%%%%%%%%%%%%%%%%%%%%
```

A.3   OTI- Optimal computation's script

```
%%%%%%%%%%%%%% Script: optimal_value.m %%%%%%%%%%%%%%%%%%
%% Optimization using CVX from Standford

%% COMMON VARIABLES%%%
M=4; % modulation level (4,8,16 QAM)
K=512; % number of channels (128,256,512,1024,2048)
```

```
Kp=64; % number of additional active subbands
Ns=2*K;
ldM=log2(M);

Nd=K; % total number of data symbols to be tx (mult. of K)
Nb=Nd*log2(M); % number of bits in packet
n=Kp;%number of tones to be computed

%%%% MODULATION %%%%%%
f1=10000; % first carrier (2f0>B:ok)
fs=96000; % sampling freq. (Jim's)
Up= exp(j*2*pi*f1/fs*(0:8*K-1)).';
%%%%%%%%%%%%%%%%%%%%%%%%

%% Variables to do the IFFT
 E = exp(j*2*pi/(8*K)*(0:(8*K-1))'*[1:K]);
 Q = exp(j*2*pi/(8*K)*(0:(8*K-1))'*[K+1:K+Kp]);

%% RUN Program %%
for z=1:100


b=pn(16,Nb,z); % binary (0,1) information sequence
Bb=reshape(b,ldM,Nd); % ldM bit streams;
d=grmap4psk(Bb);

x = E*d.';

s=real(x.*Up);
old(z)=10*log10( compute_PARP(s.',s.') );



cvx_begin
    variable c(n) complex;
    minimize( norm( real( (-Q*c + x).*Up ), Inf) ) ;
cvx_end

new(z)=10*log10( compute_PARP( real( ( (-Q*c+x).*Up).'),s.'));



end
%% PLOT THE RESULTS %%


[N,X]=hist(new)
[N0,X0]=hist(old)
figure(1)
semilogy(X0,1-cumsum(N0)./sum(N0),'b',X,1-cumsum(N)./sum(N),'r')
figure(1), legend('without tone insertion', 'optimal tone insertion')
xlabel('PAR_0 (dB)')
ylabel('Pr(PAR>PAR_0)')
```

```
Y=real(x);
Y2=real(x-Q*c);
subplot(2,2,3), plot( [1:(2*length(Y)+1)].*2*pi/(2*length(Y)+1) , 10*log10(abs(fft(xcorr(Y,length(Y))  )
subplot(2,2,1), plot(Y), axis([0 9000 -70 70]), ,xlabel('Sample'), ylabel('Amplitude')
subplot(2,2,4), plot( [1:(2*length(Y2)+1)].*2*pi/(2*length(Y2)+1) , 10*log10(abs(fft(xcorr(Y2,length(Y2)
subplot(2,2,2), plot(Y2), axis([0 9000 -70 70]), ,xlabel('Sample'), ylabel('Amplitude')
%%%%%%%%%%%%%%%%%%%%%%%%%%%%%%%%%%%%%%%%%%%%%%%%%%%%%
```

A.4   Auxiliary scripts

```
%%%%%%%%%%%%%%%% Script: pn.m %%%%%%%%%%%%%%%%%%%
%%%Generating Radom Sequences to test the algorithms %%%

function b=pn(m,Nb,Nb0); % binary (0,1) m-register sequence of length Nb, shifted by Nb0. The original s


eval(['load pn',int2str(m)]);
bb=[];
for i=1:ceil(Nb/(2^m-1))+1;
    bb=[bb b];
end;
b=bb(1+Nb0:Nb+Nb0);



%%%%%%%%%%%%%%%% Script: grmappsk.m %%%%%%%%%%%%%%%%%%%
%% Computing the 4PSK Modulation %%%

function d=grmap4psk(B);

[L,Nd]=size(B);
if L~=2; disp('wrong size'); end;

Bpm=1-2*B;
for n=1:Nd;
    x=Bpm(:,n);
    d(n)=x(2)+j*x(1);
end;
d=d/sqrt(2);



%%%%%%%%%%%%%%%% Script: compute_PARP.m %%%%%%%%%%%%%%%%%%%
function paprSymbol=compute_PARP(u,u0)

u=real(u);
u0=real(u0);

%
meanSquareValue = u0*u0'/length(u0);
peakValue = max(u.*conj(u));
paprSymbol= peakValue/meanSquareValue;
```

```
% % u=resample(u,4,1);
% % u0=resample(u0,4,1);
% %%%%L=1%%%%%
% a=max(abs(u))^2;
% paprSymbol=a/pwr(u0);

%%%%L=4%%%%%
%We resample in order to compute the real value PARP in the analog signal
%Y2=resample(u,4,1);
%PAPR_L_4=10*log10(max(abs(Y2))^2/(pwr(Y2)));

%%% The difference after oversampling%%%
%diff=PAPR_L_4-PARP_L_1;



end

function p=pwr(x);
p=sum(abs(x).^2)/length(x);
end
```

Bibliography

[1] J. Tellado, "Multicarrier modulation with low PAR: applications to DSL and wireless," *Phd Stanford dissertation*, vol. 1, no. 1, pp. 65–92, April 2000.

[2] A. Jayalath and C. Tellambura, "Reducing the peak-to-average power ratio of orthogonal frequency division multiplexing signal through bit or symbol interleaving," *Electronics Letters*, vol. 36, no. 13, pp. 1161–1163, Jun 2000.

[3] R. E. Williams and H. F. Battestin, "Coherent recombination of acoustic multipath signals propagated in the deep ocean," *The Journal of the Acoustical Society of America*, vol. 50, pp. 1433–1442, 1971.

[4] M. Chitre, S. Shahabudeen, L. Freitag, and M. Stojanovic, "Recent advances in underwater acoustic communications & networking," in *OCEANS 2008*, Sept. 2008, pp. 1–10.

[5] A. Baggeroer, "Acoustic telemetry–an overview," *Oceanic Engineering, IEEE Journal of*, vol. 9, no. 4, pp. 229–235, Oct 1984.

[6] M. Stojanovic, "Recent advances in high-speed underwater acoustic communications," *Oceanic Engineering, IEEE Journal of*, vol. 21, no. 2, pp. 125–136, Apr 1996.

[7] M. Stojanovic and J. Preisig, "Underwater acoustic communication channels: Propagation models and statistical characterization," *Communications Magazine, IEEE*, vol. 47, no. 1, pp. 84–89, January 2009.

[8] M. Stojanovic, "Low complexity OFDM detector for underwater acoustic channels," in *OCEANS 2006*, Sept. 2006, pp. 1–6.

[9] ——, "On the relationship between capacity and distance in an underwater acoustic channel," *Proc. First ACM International Workshop on Underwater Networks (WUWNet)*, Sept. 2006.

[10] B. Li, S. Zhou, M. Stojanovic, L. Freitag, and P. Willett, "Multicarrier communication over underwater acoustic channels with nonuniform doppler shifts," *Oceanic Engineering, IEEE Journal of*, vol. 33, no. 2, pp. 198–209, April 2008.

[11] G. Wunder and H. Boche, "Peak value estimation of bandlimited signals from their samples, noise enhancement, and a local characterization in the neighborhood of an extremum," *Signal Processing, IEEE Transactions on*, vol. 51, no. 3, pp. 771–780, March 2003.

[12] C. Tellambura, "Computation of the continuous-time PAR of an OFDM signal with BPSK subcarriers," *Communications Letters, IEEE*, vol. 5, no. 5, pp. 185–187, May 2001.

[13] S. H. Han and J. H. Lee, "An overview of peak-to-average power ratio reduction techniques for multi-carrier transmission," *Wireless Communications, IEEE*, vol. 12, no. 2, pp. 56–65, April 2005.

[14] M. C. Jeruchim, P. Balaban, and K. S. Shanmugan, *Simulation of communication systems*. New York, NY, USA: Plenum Press, 1992.

[15] R. O'Neill and L. Lopes, "Envelope variations and spectral splatter in clipped multicarrier signals," *Personal, Indoor and Mobile Radio Communications, 1995. PIMRC'95. 'Wireless: Merging onto the Information Superhighway'., Sixth IEEE International Symposium on*, vol. 1, pp. 71–75 vol.1, Sep 1995.

[16] X. Li and J. Cimini, L.J., "Effects of clipping and filtering on the performance of OFDM," *Communications Letters, IEEE*, vol. 2, no. 5, pp. 131–133, May 1998.

[17] D. Dardari, V. Tralli, and A. Vaccari, "A theoretical characterization of nonlinear distortion effects in OFDM systems," *Communications, IEEE Transactions on*, vol. 48, no. 10, pp. 1755–1764, Oct 2000.

[18] A. Jones, T. Wilkinson, and S. Barton, "Block coding scheme for reduction of peak to mean envelope power ratio of multicarrier transmission schemes," *Electronics Letters*, vol. 30, no. 25, pp. 2098–2099, Dec 1994.

[19] A. Jones and T. Wilkinson, "Combined coding for error control and increased robustness to system nonlinearities in OFDM," in *Vehicular Technology Conference, 1996. 'Mobile Technology for the Human Race'., IEEE 46th*, vol. 2, Apr-1 May 1996, pp. 904–908 vol.2.

[20] A. E. M. I. M. A. I. A. Ashraf A. Eltholth, Adel R. Mikhail, "Peak-to-average power ratio reduction in OFDM systems using huffman coding," *PWASET*, vol. 33, pp. 266–270, SEPTEMBER 2008.

[21] S. Muller and J. Huber, "OFDM with reduced peak-to-average power ratio by optimum combination of partial transmit sequences," *Electronics Letters*, vol. 33, no. 5, pp. 368–369, Feb 1997.

[22] ——, "A novel peak power reduction scheme for OFDM," in *Personal, Indoor and Mobile Radio Communications, 1997. 'Waves of the Year 2000'. PIMRC '97., The 8th IEEE International Symposium on*, vol. 3, Sep 1997, pp. 1090–1094 vol.3.

[23] A. D. S. Jayalath and C. Tellambura, "Adaptive pts approach for reduction of peak-to-average power ratio of OFDM signal,," *Elect. Lett.*, vol. 36, pp. 1226–1228, July 2000.

[24] R. Bauml, R. Fischer, and J. Huber, "Reducing the peak-to-average power ratio of multicarrier modulation by selected mapping," *Electronics Letters*, vol. 32, no. 22, pp. 2056–2057, Oct 1996.

[25] P. Van Eetvelt, G. Wade, and M. Tomlinson, "Peak to average power reduction for OFDM schemes by selective scrambling," *Electronics Letters*, vol. 32, no. 21, pp. 1963–1964, Oct 1996.

[26] B. Krongold and D. Jones, "PAR reduction in OFDM via active constellation extension," *Broadcasting, IEEE Transactions on*, vol. 49, no. 3, pp. 258–268, Sept. 2003.

[27] R. Prabhu and E. Grayver, "Active constellation modification techniques for OFDM PAR reduction," in *Aerospace conference, 2009 IEEE*, March 2009, pp. 1–8.

[28] A. Aggarwal and T. Meng, "Minimizing the peak-to-average power ratio of OFDM signals using convex optimization," *Signal Processing, IEEE Transactions on*, vol. 54, no. 8, pp. 3099–3110, Aug. 2006.

[29] B. Krongold and D. Jones, "An active-set approach for OFDM PAR reduction via tone reservation," *Signal Processing, IEEE Transactions on*, vol. 52, no. 2, pp. 495–509, Feb. 2004.

[30] S. Janaaththanan, C. Kasparis, and B. Evans, "A gradient based algorithm for PAPR reduction of OFDM using tone reservation technique," in *Vehicular Technology Conference, 2008. VTC Spring 2008. IEEE*, May 2008, pp. 2977–2980.

[31] J. Ilic and T. Strohmer, "PAPR reduction in OFDM using Kashings representation," *IEEE*, pp. 444–448, 2009.